LOAD BALANCING AS A DESIGN METHOD

FOR CONCRETE PRESTRESSED BRIDGE GIRDERS

By

LANCE R. LUKE

Bachelor of Science in Architectural Engineering

Oklahoma State University

Stillwater, Oklahoma

2012

Submitted to the Faculty of the
Graduate College of the
Oklahoma State University
in partial fulfillment of
the requirements for
the Degree of
MASTER OF SCIENCE
December, 2016

LOAD BALANCING AS A DESIGN METHOD

FOR CONCRETE PRESTRESSED BRIDGE GIRDERS

Thesis Approved:

Bruce Russell, PhD

Thesis Adviser

Tyler Ley, PhD

Steven O'Hara, MS

John Philips, MS

ACKNOWLEDGEMENTS

Thanks to my professors for the encouragement to pursue my thesis. And many thanks to all my friends and family that supported me through this process.

Name: LANCE R. LUKE

Date of Degree: December, 2016

Title of Study: LOAD BALANCING AS A DESIGN METHOD FOR CONCRETE PRESTRESSED BRIDGE GIRDERS

Major Field: CIVIL ENGINEERING

Abstract: Load balancing is a design method for prestressed structural members, primarily beams and slabs, that provides efficient use of materials. When using load balancing, the prestressing tendon is designed for a prestressing force and eccentricity in order to 'balance' all or a portion of the dead load. Commonly the procedure is used for post-tensioned cast in place structures. However, it is not used typically for precast, pre-tensioned members. Instead, current design methods focus on the ultimate design strength and allowable stresses at service loads, which can provide inefficient use of prestressing force. This "inefficient" prestress force can cause many complications for prestressed members, such as excessive cracking in the end regions, uncontrolled amounts of camber after release, and inefficient use of materials. Although ultimate strength and allowable stress design methods are important for safety, they provide a design that rarely experiences the full extent of the loads applied. Designing a prestressed member by balancing dead load will provide a more efficient design that is also safe. Creating a uniform compression force of the concrete member under dead load is the goal for the load balancing method. Uniform prestressing forces necessary for the load balancing will greatly reduce the amounts of end cracking, control camber and deflection, and limit the waste of material. Mild steel can be added to the member to meet modern design codes, ensure strength of the member and control cracking for un-balanced load. Load balancing as a design method should be considered for an efficient pretensioned concrete member design to reduce many problematic issues associated with modern bridge girders.

TABLE OF CONTENTS

Chapter Page

I. INTRODUCTION 1

II. REVIEW OF LITERATURE AND BACKGROUND 8

Load-Balancing Method for Design and Analysis of Prestressed Concrete Structures 8
Evaluation of crack control methods for end zone cracking in prestressed concrete bridge girders 11
Precast, prestressed girder camber variability 14
Serviceability Based Design of Partially Prestressed Beams 16
Non-tensioned Steel in Prestressed Concrete Beams 18
Fatigue Testing of Two Full-Size Pre-Cracked AASHTO Bridge Girders 20
Background and Supporting Information 22

III. METHODOLOGY 44

Outline 44
Concrete Section and Material Properties 46
Bridge Loads 47
Loss Calculations 49
Preliminary Load Balance Calculations 51
Strand Calculations 51
Stress Calculations 52
Debonding Calculations 53
Ultimate Strength Calculations 54
Camber and Deflection Estimates 54
Other Serviceability Concerns 55

Chapter Page

IV. PRESENTATION OF RESULTS 57

Introduction 57
Type IV Girder Design Comparison 57
ODOT Design 60
Load Balance beam weight only design 65
Load Balance beam weight and 50% slab 69
Load Balance beam weight and 75% slab 73
Load Balance beam weight and 100% slab 77

V. CONCLUSION 84

Introduction 84
Design Summary 84
Conclusion 84

VI. RECOMMENDATIONS 86

REFERENCES 87
APPENDICES

LIST OF TABLES

Table Page

1.....24
2.....24
3.....25
4.....25
5.....26
6.....26
7.....28
8.....29
9.....40
10.....43
11.....82

LIST OF FIGURES

Figure Page

1.....2
2.....5
3.....6
4.....6
5.....7
6.....12
7.....23
8.....30
9.....30
10.....36
11.....36
12.....38
13.....41
14.....46
15.....58
16.....60
17.....62
18.....63
19.....65
20.....67
21.....68
22.....69
23.....71
24.....72
25.....73
26.....75
27.....76
28.....77
29.....79
30.....80

LIST OF NOTATIONS

Notation Definition

β_1 .....Ratio of the depth of the Whitney stress block to the depth of the neutral axis
Σ_o..... Sum of reinforcing elements' circumferences
γ..... Concrete unit weight
γ_e..... Exposure factor
γ_p.....Prestressing steel type factor
Δ.....Deflection (-) or camber (+) of member
Δf_s.....Net stress in the prestressed tendon at any load level in which the decompression load
..... is taken as the reference point
ρ .....Ratio of mild tension steel area to gross section area
ρ' ..... Ratio of mile compression steel area to gross section area
ρ_p .....Ratio of prestressing area to gross section area
φ ..... Curvature of member
A..... Area of member section
A..... Effective concrete area per bar
A_{ps} ..... Area of prestressing steel
A_s.....Area of mild steel
A_t.....The effective concrete area in uniform tension
a.....Depth of Whitney stress block (0.85*c)
b .....Width of member section
CR .....Creep losses
c.....Depth of compression block, distance from extreme compression fiber to neutral axis
DC.....Dead load component
d_c.... Thickness of concrete cover measured from extreme tension fiber to the center of
..... the flexural reinforcement located closest thereto
d_l.....Distance from the extreme compression fiber to a centroid of extreme tension steel
.....element
d_p..... Depth from extreme compression fiber to center of prestressing strands
d_s .....Depth from extreme compression fiber to center of mild steel
E_c .....Modulus of elasticity of concrete at 28 days
E_{ci} , E_{ct}.....Modulus of elasticity of concrete at 7 days
E_{ps} .....Modulus of elasticity of prestressing strand
E_s..... Modulus of elasticity of mild steel reinforcing
ES ..... Elastic shortening losses
F ..... Prestressing force
F_p..... Prestressing force
f..... Member stress
f_b ..... Stress at bottom of member section

f'_c ..... Concrete compressive strength at 28 days
f'_{ci} ..... Concrete compressive strength at 7 days
f_{min} ..... Minimum live load stress resulting from Fatigue 1 load combination, combined with the more severe stress from either the permanent load or the permanent loads, shrinkage, and creep-induced external loads; Positive if tension, negative if compression
f_{pe} ..... Stress from prestressing forces
f_{ps} ..... Prestressing stress
f_{pt} ..... Stress of prestressing strand
f_{pu} ..... Ultimate steel stress
f_r ..... Rupture stress (7.5sqrtf'c)
f_{ss} ..... Tensile stress in steel reinforcement at the service limit state
f_t ..... Stress at top of member section
f_y ..... Steel yielding stress
h ..... Eccentricity from the center of gravity of concrete member to the center of gravity of the prestressing strands
h ..... Overall depth of member section
I ..... Moment of inertia
I_{cr} ..... Cracked moment of inertia
I_e ..... Effective moment of inertia
I_g ..... Gross moment of inertia
IM ..... Dynamic load factor
K_g ..... Stiffness of member, i.e. moment of inertia
L ..... Length of member
LL ..... Live load
l ..... Span of member
M_a ..... Actual applied moment
M_{cr} ..... Cracked moment of inertia
M_g ..... Gravity moment
m ..... Multi-presence factor
PPR ..... Partial prestressing ration
p ..... Multi-presence factor for fatigue
RE ..... Relaxation losses
S ..... Section modulus
S ..... Spacing of bridge girders
S' ..... Composite section modulus
SH ..... Shrinkage losses
T ..... Tension force
TL ..... Total losses
t_s ..... Thickness of concrete bridge deck

w ..... Uniform distributed load
w ..... Crack width
x ..... Distance from end of member to a specified location
y ..... Distance from extreme fiber to center of gravity of member section
y_t ..... Distance from center of gravity of member to top of section

CHAPTER I

INTRODUCTION

Precast, prestressed beams can encounter severe serviceability concerns such as excessive cambers, cracking caused by unbalanced tensile stresses, and various problems associated with the application of large prestressing forces near the end regions of precast, prestressed concrete beams. A prestressed member designed for high loadings produces high prestressing forces. When large prestressing forces occur, concern for serviceability increases. High prestressing stresses can induce unnecessary camber and the large amount of camber can cause problems with deck construction. These large prestressing forces in turn can cause large amounts of unbalanced tension stressed in end regions, which then cause cracking. Cracking is a huge serviceability and durability issue. If the cracking is not controlled or mitigated, it could lead to the intrusion of damaging water borne salts, which in turn can lead to the corrosion of steel within the prestressed members. Excessive cracking may also cause prestressing strands to debond, which greatly reduces the member's structural integrity.

Prestressing concrete is an effective use of material because concrete is strong in compression whereas steel is much stronger in tension. The purpose of prestressing a concrete member is to counteract the tensile stresses created from loading by internally compressing the member. Simple beam mechanics and material science apply to prestressed members. These simple principles are required in order to find the amount of prestress required from load

balancing via shear and moment diagrams, the stresses at the top and bottom of the cross section, and the ultimate strength of the member. Compressive stresses and tensile stresses are imparted onto the concrete from axial prestressing, external moments, and internal moments. The various external sources are: permanent loads that impart a dead load moment, fluctuating loads that create a live load moment, and prestressing forces that create a moment from the eccentricity of the force and centroid and a uniform compressive strength. Stresses from the gravity moments can be found by $f = M_g/S$ (simplified with $S = I/y$) (Design of Prestressed Concrete Structures, p. 134), compressive stresses from prestressing forces by $f = F_p/A$ (Design of Prestressed Concrete Structures, p. 127), and stresses from prestress eccentricity by $f = F_p \times e/S$ (simplified with $S = I/y$) (Design of Prestressed Concrete Structures, p. 129). The diagram below shows the use of these basic principles.

Figure 1 - (Design of Prestressed Concrete Structures)

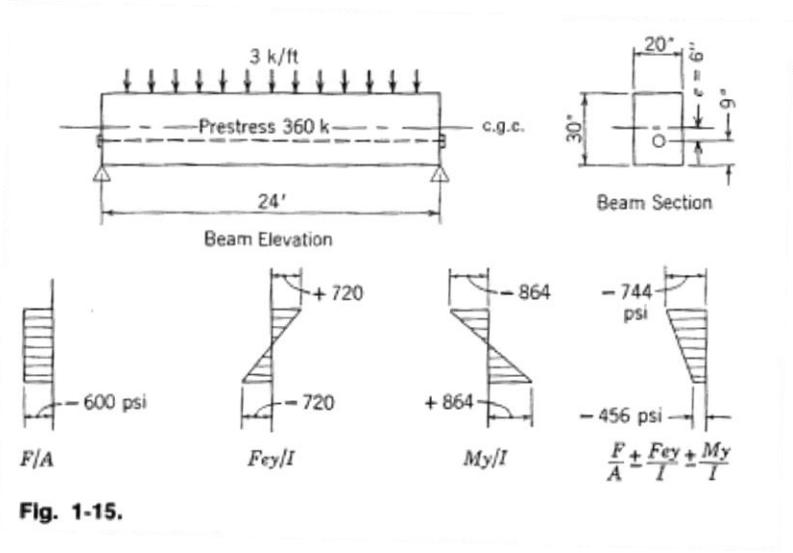

Load balancing involves resisting the design moment by draping the prestressing strands in a parabolic pattern to mimic the moment diagram. This ensures the member only resists the moment found at that particular section of the member. Thus at the ends, where no moment is found at a simple span, the eccentricity is zero and at the midspan where moment is maximum the

eccentricity is maximum. However, it is common practice to use straight strands and debond strands in order to create a similar effect without draping. If draped or harped strands are desired the amount of strands should be limited only to meet the desired eccentricity. The simplicity of load balancing lends itself as the most effective design method.

For load balancing, uniform compression is ideal, and the F/A stress is ignored (because it is uniform compression) which leaves $\frac{Fe}{S} = \frac{M}{S}$. This reduces to $Fe = M$. The prestressing force and eccentricity should counteract the applied dead load (or portion thereof) to achieve a uniform compressive stress throughout the member. This should be true for the length of the member, thus a draped pattern (to match the parabolic moment diagram) would be ideal. Design for a simple span prestressed member for load balancing is straight forward: a simple span member under uniform load the amount of drape required from load balancing is

$h = (wL\text{^}2)/8F$ (Lin & Burns, p. 395).

A more complex design involving a prestressed beam and composite deck is shown next, which provides the basis for bride girder design by the load balancing method. To begin, a simple prestressed rectangular beam is considered for a load balance design. First, assume the beam self-weight moment, M_b, is the same as the bridge deck self-weight, $M_b = M_s$, and the vehicular live load is twice the beam self-weight, $M_L = 2.0\ M_b$. These are reasonably assumptions for a typical bridge design. [For example, an AASHTO Type IV bridge girder spanning 100'-0" spaced at 8'-3". The self-weight for a Type IV girder with normal weight concrete is w_b=0.822 klf. The weight of the 8" concrete deck is w_s=0.825 klf, thus the beam weight and slab weight are approximately the same, $w_b = w_s$. The live load for HS20 truck is 1.219 klf, the lane load is 0.640 klf, and with the impact factor (33%) and distribution factor (0.73) the total live load is w_L=1.662klf which is approximately twice the beam self-weight, $w_L = 2.0w_b$.]

Load balancing for a simple rectangular prestressed beam for just the beam self-weight is one possibility for load balancing. A rectangular beam with a depth of h, width of b, and depth of the prestressing force 3/4h then prestressing force required to balance the self-weight and create a uniform compressive stress is as follows: M_p=M_b, $\frac{F_p \times e}{S} = \frac{M_b}{S}$. The stress due to prestress compression is $\frac{-F_p}{A}$ and the stress of the eccentric prestress force is $\pm\frac{F_p \times e}{S}$ or $\pm\frac{1.5F_p}{A}$. The stress due to beam self-weight is $\frac{M_b}{S}$, using $M_b = \frac{F_p \times h}{4}$, the stress becomes $\pm\frac{1.5F_p}{A}$. The stresses at midspan of the girder at release for the top and bottom are $f_{top} = f_{bot} = \frac{-F_p}{A}$. The stresses at the ends during release are $f_{top} = \frac{0.5F_p}{A},\ f_{bot} = \frac{-2.5F_p}{A}$. When the slab is cast the applied dead load doubles so the stresses at midspan become: $f_{top} = \frac{-2.5F_p}{A},\ f_{bot} = \frac{0.5F_p}{A}$. The stresses at the ends remain the same because the uniform loading bending stresses are zero.

Load balancing the section for the total dead load (the beam weight and slab weight) is another option for a prestressed girder. Since the dead load to be balanced is doubled the prestressing force will be doubled. The beam weight bending moment, keeping the eccentricity the same, is $M_b = \frac{F_p \times h}{8}$, which makes the beam weight bending stresses $\pm\frac{0.75F_p}{A}$. The stresses during release at midspan are: $f_{top} = \frac{-0.25F_p}{A},\ f_{bot} = \frac{-1.75F_p}{A}$. There is only compression at release but it is not uniform. The stresses at release at the ends of the member are $f_{top} = \frac{0.5F_p}{A},\ f_{bot} = \frac{-2.5F_p}{A}$. Once the concrete slab is cast into place the self-weight is doubled and thus equalizes the bending stresses from the eccentric prestress force. The uniform stress from the prestress force is the resultant stress, $f_{top} = f_{bot} = \frac{-F_p}{A}$. The stresses at the ends remain the same.

Once the slab has been cured and hardened a composite section can be utilized. Assuming the deck is h/6 deep and 6b wide the following properties can be formed: $c_b = \frac{19}{24}h$, $I_x = \frac{221}{864}bh^3$, $S_b = \frac{221}{684}bh^2$, and $S_t = \frac{221}{324}bh^2$.

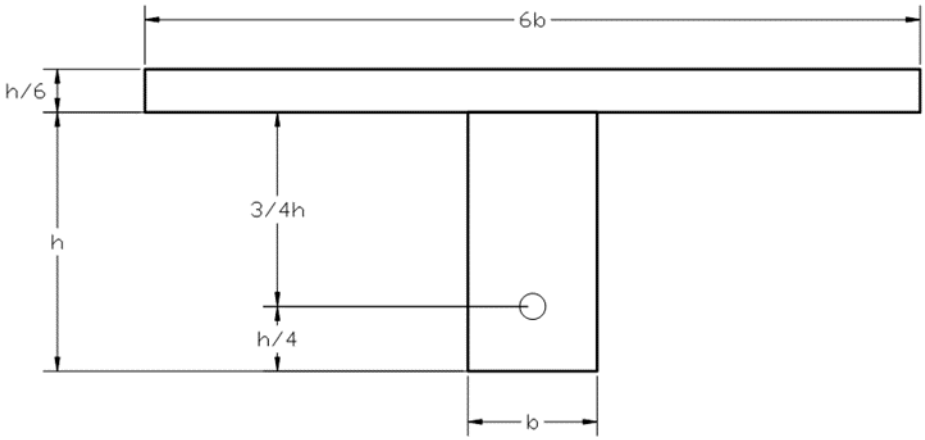

Figure 2-General Rectangular Prestressed Beam with Composite Decking

With the live load twice the beam self-weight (M_L=2.0M_b) the stresses increase accordingly. The stresses created from the live load for load balancing of the beam weight only is $f_{top} = \frac{-162F_p}{221A}$, $f_{bot} = \frac{342F_p}{221A}$. The midspan stresses (at beam) for load balancing of the beam weight only become: $f_{top} = \frac{-1285F_p}{442A}$, $f_{bot} = \frac{905F_p}{442A}$. The stresses created from the live load for load balancing of the total dead weight is $f_{top} = \frac{-81F_p}{221A}$, $f_{bot} = \frac{171F_p}{221A}$. The midspan stresses (at beam) for load balancing of the total dead weight only become: $f_{top} = \frac{-266F_p}{221A}$, $f_{bot} = \frac{-50F_p}{221A}$. The stress diagrams for both methods of load balancing are shown in Figures 3 and 4. This simplistic model reveals that load balancing for the total dead load is more effective in reducing the total final stresses. This is shown by the uniform compression stress during the total dead load application and the compressive stresses present during live load applications. This simplistic model ignores effects from prestress losses and allowable concrete stresses which shall be checked for code

compliance, which may require slight adjustments of the prestressing, debonding, or addition of mild steel.

Figure 3-Midspan stresses of a prestressed rectangular beam, balanced for beam weight only

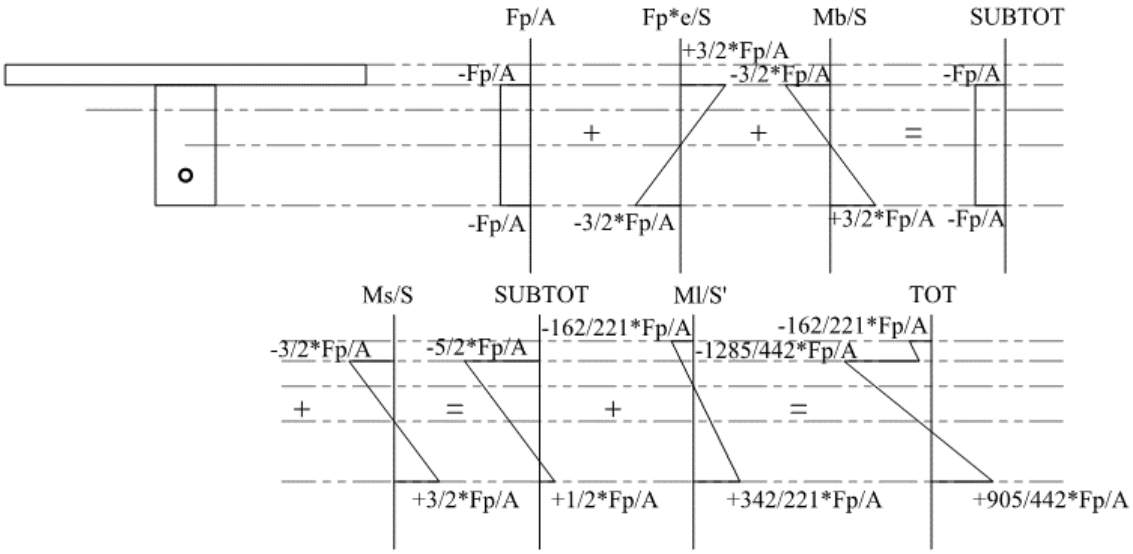

Figure 4-Midspan stresses for prestressed rectangular beam, balanced for beam and deck

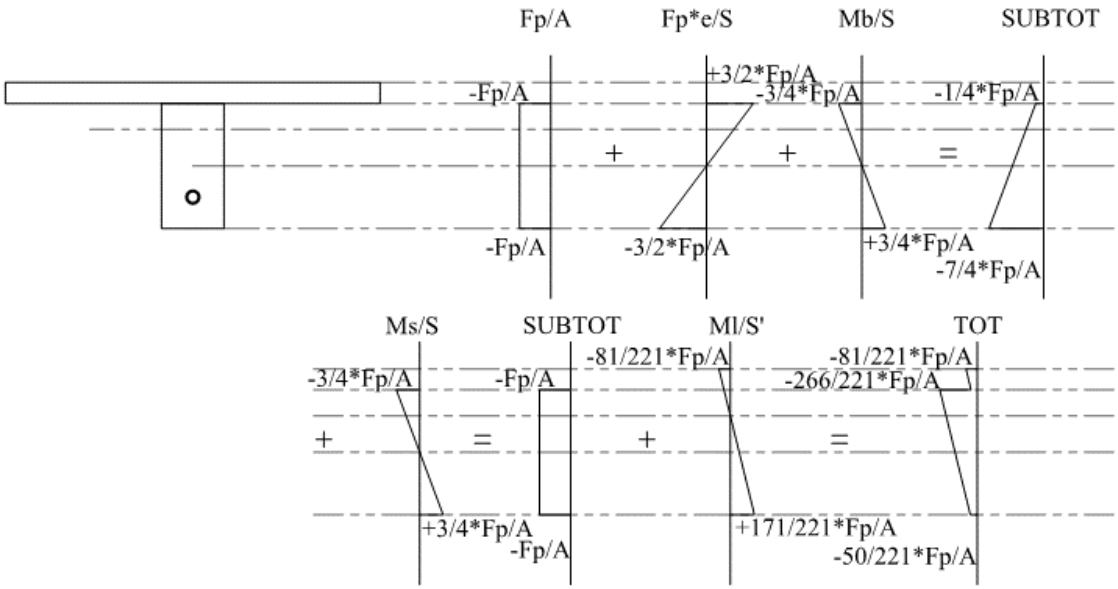

Figure 5-End stresses for prestressed rectangular beam

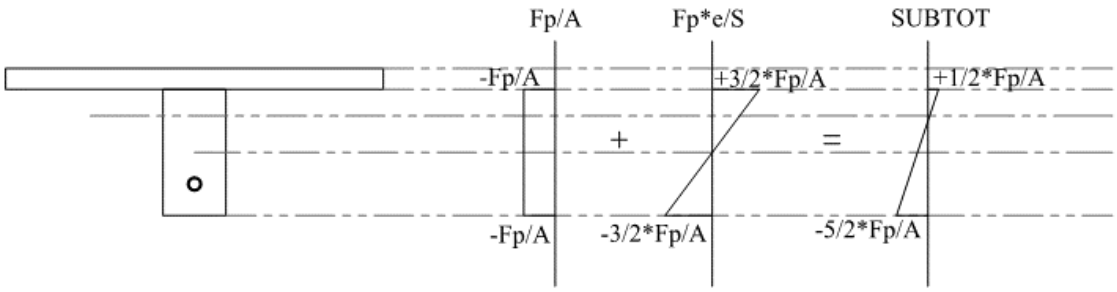

This thesis explores the possible methods by which load balancing principles can be applied to precast, pretensioned beams with special interest in bridge girders. Exploration of the load balancing methodology for reducing serviceability concerns associated with current design methods.

CHAPTER II

REVIEW OF LITERATURE

1. Load-Balancing Method for Design and Analysis of Prestressed Concrete Structures by T.Y. Lin

The load balancing, proposed by T.Y. Lin, is an alternate design method to the ultimate design strength method and the working stress method. For load balancing, dead load moments (or a portion of the dead load moments) are resisted by an eccentric prestressing force. This prestressing force should be applied to match that of the dead load moment diagram. For post-tensioned members the draping can be easily achieved. However, draping is much more difficult for precast, pretensioned members. This thesis explores the possible methods by which load balancing principles can be applied to precast, pretensioned beams with special interest in bridge girders.

The ultimate design method uses a factored applied load and a Whitney stress block to oppose the factored load. The working stress method uses an unfactored applied load, so that the maximum tensile stress of the concrete member does not exceed the concrete stress believed to induce cracking. The basic principle of load balancing is to apply a prestressing force to counteract the load imposed on the member- usually unfactored dead load and a small portion of the live load. Ideally this method puts a uniform compression load throughout the member. However, most prestressed members must be designed for a variable live load that is not

permanently applied to the member. Typically, the load balancing should cancel out all of the permanently applied dead loads and some portion of the live load (usually a small portion, 0 to 20%). This load balancing method counteracts the load that the member resists throughout the entire life span, which is more desirable than resisting loads not encountered over a majority of its lifespan. Lin states, “Since the balanced-load point is often indicative of the behavior during the greater portion of the life span of a prestressed structure, it could deserve more consideration than either the working load or the ultimate load.” (p. 723)

At the point of load balancing there will be no deflections or bending due to the uniform compression in the member. So, this allows for the remaining live load to be checked easily. This additional load must be checked to make sure the allowable stresses are not exceeded. To balance a uniform load the prestressing strands are draped to the parabolic shape of the moment diagram. The amount of the midspan drape depends on the amount of prestressing force used to counteract the bending moment, as shown below (equation has been rearranged).

$h = \frac{wL^2}{8F}$ (p. 721)

This idea of load balancing not only designs, but also analyzes the beam in the same manner. This is because at every instance along the member, the eccentricity of the strands creates an internal moment that offsets the applied moment. So, the member would only need to be checked for any added live load that it may experience. To resist this additional live load (which has not been balanced) non-prestressed reinforcing can be utilized. This same method can be applied to cantilever beams and continuous beams. The strands again follow the parabolic shape of the moment diagram. Load balancing is an effective design method to increase the efficiency of prestressed members.

This idea is the basis for an economical prestressed member design. Simple prestress design procedures can be implemented to resist sustained loads, while the addition of non-

tensioned steel can resist any additional temporary load if the stresses exceed the allowable stresses.

2. Evaluation of crack control methods for end zone cracking in prestressed concrete bridge girders by Pinar Okumus and Michael G. Oliva

End region cracking is a serviceability concern often found in I-shaped prestressed bridge girders. End region cracks occur during the release of prestressing strands and are potential sites for chloride infiltration. This type of infiltration causes deterioration of the strands and shortens the service life of the bridge. Stated by the authors, “The cracking appears to be more severe in recently developed deeper sections with slender webs and larger amounts of prestress,” (p. 91). When, focusing on end region detailing, cracking can become nonexistent or minimized.

The cracks follow certain paths due to various reasons. The authors offer these opinions about potential crack profiles and cause:

1) Horizontal web cracks caused by the eccentricity of the strands over the depth of the section
2) Inclined cracks caused by draping of the strands
3) Bottom flange Y-cracks caused by the high amount of prestressing force in the bottom flange
4) Vertical transverse cracking in the bottom flange is also common but not a part of this report (created from casting bed).

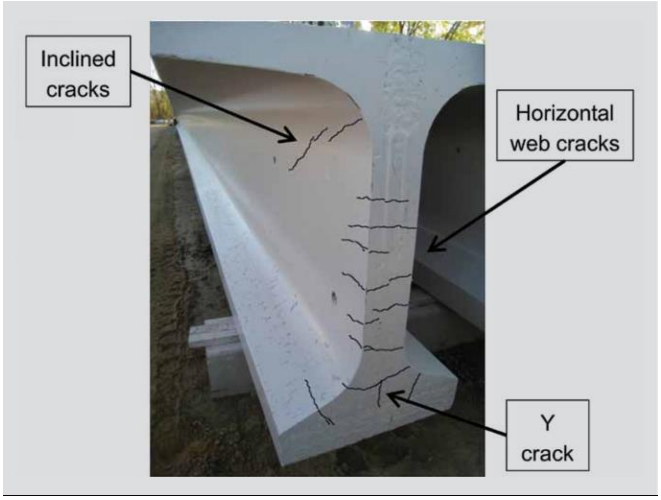

Figure 6-Types of Cracking

The authors conducted an experiment involving the construction of multiple full scale specimens. The experiment involved a 54 in. deep flanged bulb-tee girder that spanned 129 feet. The end regions were modeled by a finite element software to compare the model to actual members. Various methods were used in order reduce end cracking. The methods utilized were:

1) Changing the flame strand cutting order
2) Removing and lowering draped strands to achieve various slopes
3) Modifying end-zone reinforcement by changing spacing and size
4) Debonding the prestressing strands by varying the amount and lengths of debonding.

By flame cutting the innermost strands first, the width of Y-cracking was reduced. Lowering and spreading the draped strands proved to reduce the inclined cracking, but reducing the draped strands often lowers the capacity of the girder due to the reduction of bottom flange strands to meet stress limitations. Increasing web reinforcement at the two sets closest to the end minimized the crack widths at the end but did not eliminate them. Debonding greatly reduced, and even eliminated all types, of cracking depending on the amount and length of debonding. The most effective method that eliminated all cracking was the combination of debonding and increasing

reinforcement size at end regions. Increasing the web reinforcement at end regions outside of the two end sets proved ineffective at reducing cracking.

There are multiple methods to decrease the end region cracking and cracking widths for prestressed pretensioned members. In combination with these methods, it is clear that if there was a lower prestressing force present the cracking would decrease.

3. Precast, prestressed girder camber variability

by Maher K Tadros, Faten Fawzy, and Kromel E. Hanna

Camber is an increasingly growing serviceability issue associated with prestressed girders. It is a highly variable effect caused by unbalanced prestressed forces. Camber is dependent on many factors all of which can create significant variations in the amount of camber one observes. These factor include concrete modulus (often tied to concrete strength), age at de-tensioning, lifting and handling, bearing locations during temporary storage, and estimated prestress losses. All of these factors can create variations in camber that must then be accounted for during deck construction. With new materials being developed, high performance (high strength) concrete can allow more prestressing to be applied, and allow for longer spans with slenderer members. The higher prestressing forces coupled with the more slender members create larger amounts of camber that cause construction problems with the decking and serviceability. Because the amount of camber has important consequences on the construction of the bridge deck, it is important to be as accurate as possible when calculating the camber (not over- or under-estimated).

There are many factors that can affect camber both initially and long term. Consideration of these variables should be included in camber estimation. These factors for initial camber are high/low modulus of elasticity of concrete, softness of aggregates, assumed initial prestress force and gross section properties, debonding and transfer lengths, and storage lengths at the plant. Each of these can affect the calculation of camber (which is quite variable). Each of these parameters either overestimated or underestimated the amount of camber against a baseline girder. Some of the more important additional factors that affect long term camber are long term loss calculations, time before deck construction, long term creep, varying elastic modulus, and deflections from dead load during construction.

For initial camber calculations, the variability of the modulus of elasticity can vary $\pm$22% of the mean value, which can greatly vary the calculated camber. Other factors that affect the modulus of elasticity are the types of aggregates used. For example, "In Florida, the use of soft native limestone rock is frequent enough to have a standard recommendation to use a 0.9 factor," in order to reduce the modulus (p. 143). Also, the designer does not have control of when the prestressing strands are released, in which the modulus can, "can change dramatically in a short period," (p. 143). Accurate prestress forces must also be calculated, thus the most accurate methods and release methods must be utilized. The length used for calculations is also important; the full length, the final span length, and storage length are all choices to be considered. The moment of inertia can also influence the camber calculations: the gross properties will over estimate camber while the transformed moment of inertia provides a more accurate calculation.

Properties that affect long term camber include some additional items that must be considered from initial camber calculations. The time between girder casting and erection is a variable that cannot be controlled by the designer, but a range of days can be specified by the designer to avoid girders a few days old, or girders stored for months. The time of deck placement and composite effect of the girder must also be accounted for in camber calculations.

The use of long term simplified creep coefficients and simplified prestressed loss calculations can provide inaccurate predictions of camber. The design calculations for losses, creep, and camber should be as accurate as possible. The recommended method for the losses at release and long term belong to the AASHTO LRFD specification.

4. Serviceability Based Design of Partially Prestressed Beams

by Antoine E. Naaman and Amnuayporn Siriaksorn

This paper examines beams that contain both prestressing strands and mild steel to give the member its tensile strength. This method is studied because partially prestressing gives rise to better cracking performance, deflection control, less high performance material usage, camber control, higher ductility, and even cost savings. Partial reinforced beams fall between reinforced concrete beams (which crack under dead load) and fully prestressed beams (which do not crack under service dead and live loads). Partially prestressed beams crack under full live load which drastically changes the cross section properties. In order to quantify the amount of prestressing in a beam a factor dubbed the "Partial Prestressing Ratio" (PPR) is used. This factor is a simple ratio of the ultimate moment capacity that considers just the prestressing strands over the ultimate moment capacity with all steel.

$$PPR = \frac{A_{ps} f_{ps} (d_p - \frac{a}{2})}{A_{ps} f_{ps} \left(d_p - \frac{a}{2}\right) + A_s f_y (d_s - \frac{a}{2})}$$ (Eq. (2), p. 68)

Various criteria must be met or considered during the application of live loads. Including: stresses during full live load, change in stress of steel for fatigue life, crack width, camber, and susceptibility to corrosion. Predicting crack width is an important topic for partially prestressed beams because cracking occurs during service live loads.

Firstly, the member must meet the ultimate strength capacity and to some degree the minimum ductility criteria. However, for service loads the unfactored dead and unfactored live are considered, but the live load may have a reduction factor. This is due to the fact that, depending on the type of structure, the full live load may never be reached. For example, railroad loads are very consistent and thus more accurately portrayed in design, but a building may only see 50% of the live load over most of its life span. Two crack width methods are introduced from

two different authors. The first relates crack width to the idealized tensile stress in the concrete, while the second method considers the tensile stress in the steel. The maximum crack width should be compared to a code standard for a given environmental exposure. Fatigue of partially prestressed members is crucial because the section properties change once the member cracks due to the live load, in turn causing drastic stress changes in the steel and concrete. The fatigue life must be check for the concrete, prestressing steel, and the mild steel reinforcing. The fatigue stress changes must be compared to various codes for this allowable stress change. The camber and deflection calculations are straight forward; however, attention to cracking must be closely followed. For un-cracked properties the gross (or transformed) section properties should be used, and if the section is cracked, an effective moment of inertia should be used for deflection. Flexure design can be used based on simple material mechanics.

5. Non-tensioned Steel In Prestressed Concrete Beams

By A. F. Shaikh and D. E. Branson

In this report, the effects of nonprestressed reinforcing in prestressed beams were developed through a series of rectangular concrete beams. The behavior characteristics examined are as follows: camber (short and long term), loss of prestress, crack formation, and deflections under working loads and overloads. Twelve beams were fabricated with varying amounts of prestressed reinforcing and varying amounts of non-prestressed reinforcing (mild and high strength). Various experimental data and parameters were recorded throughout the procedure such as shrinkage, strength, temperature, humidity, concrete and steel strains, camber, deflection, and failure load. Theoretical calculations were made to compare with experimental data such as prestress losses, camber/deflection, and strength. Most of the theoretical calculations closely resembled experimental data. Short term camber does not change much except that the use of a transformed section is recommended in computing initial camber. However, for long term camber, modification factors were proposed to achieve a more accurate prediction. The long term camber was reduced with the use of non-prestressed reinforcing. Non-prestressed reinforcing also reduced the amount of prestress losses. Again, modification factors were proposed to account for the fact the non-prestressed steel takes some of the load during strand release. This non-tensioned steel reduces the amount of creep and shrinkage. The first instance of cracking is not influenced by the addition of non-tensioned steel. After the onset of initial cracking the non-tensioned steel greatly reduces the amount of total cracking in a prestressed member. The effects of non-tensioned steel on deflections is not as well understood as some of the other topics. Deflections are actually greater with non-tensioned steel when the load is below the cracking moment; however, the greater the load is above the cracking moment the more considerably smaller the deflections become. The ultimate load follows material mechanics with both types of steel

considered. This experiment of the utilization of non-tensioned steel is very positive and concludes that using non-tensioned steel is very useful in prestressed beams.

6. Fatigue Testing of Two Full-Size Pre-Cracked AASHTO Bridge Girders

By P. Zia, M. J. Kowalsky, G. C. Ellen, and S. E. Longo

Two bridge girders (Type III and Type V) were tested with 1,000,000 cycles of service loads and 2,500 cycles of overloads added between the service cycles. Bridge engineers had a growing concern about transverse cracks within the middle third of the concrete girders during production which prompted investigation. In a previous study, these cracks were determined to be caused by the restraint of the concrete during ambient cooling by the prestressing strand. However, once the prestressed strands were released the cracks would close and become unnoticeable. Testing was performed to determine if these cracks affected fatigue performance on typical bridge girders.

The Type III girder was 65'-5 ½" long and contained 34 prestressing strands with 22 straight strands and 12 draped strands with hold downs at 6'-1" on either side of the midspan. The Type V girder was 65' long and contained 36 straight prestressing strands. Both contained the cracks mentioned above before testing occurred. The members were simply supported by bearing pads and were initially loaded until flexural cracks occurred at the bottom flange with load deflection data compiled. Next, the members were cyclically loaded with one million service loads cycles with 500 cycles of overload after every 200,000 cycles of service loads. Deflection data was recorded after each overload cycle load, as well as the crack development data. Finally, the girders were load until failure to determine the ultimate capacity. Then the fatigue stresses were compared to NCDOT allowable design values.

The cracks under service loads were not significant. However, under overload (75% of ultimate strength) significant cracking was observed. The Type III girder experienced cracks in the middle 19' with the maximum crack length of 21.5" and crack width of 0.013" with a spacing of 5.5". The Type V girder experienced cracks in the middle 13' with the maximum crack length

of 47” and crack width of 0.025” with a spacing of 8” to 10”. Both girders remained in the elastic range during fatigue loading, suggesting the cyclic loading had no effect on stiffness, but load deflection curves suggest there was a gradual reduction in camber. Under ultimate loading, the girders maintained stiffness with significant cracking, and experienced a gradual stiffness reduction until failure.

In conclusion, after all cyclic loading there was no degradation of stiffness, strength, or ductility. However, after each 500 cycles of overloading, cracking and permanent deflection increased but prestressing strands showed no sign of failure. The stress range put forth from AASHTO proved to be a suitable allowance for bridge girders.

7. Background and Supporting Information

From various sources (ie. ACI, PCI, and AASHTO)

This chapter is provided to explain material that is used in the thesis and where that information is referenced. Most of the background information is spelled out precisely in various design codes.

Calculation of section properties are very straight forward, they follow simple statics and strength of materials. However, when cracked these properties change. When stresses lead the member to crack, different sections properties must be calculated to account for the cracking, when encountered. An effective moment of inertia can be found based upon the following equations:

$I_e = (\frac{M_{cr}}{Ma})^3 I_g + \left[1 - (\frac{M_{cr}}{M_a})^3\right] I_{cr}$ (ACI, Eq. 24.2.3.5a),

where I_{cr} is the cracked moment of inertia, and

$M_{cr} = \frac{(f_r + f_{pe})I_g}{y_t}$ (ACI, Eq. 24.2.3.9).

Cracking in a bridge girder is rare due to the large gross section properties, but in the rare case the cracking moment is exceeded the effective properties should be used for deflection.

If any loads create cracking in the member it will be the live load. Live load for bridges is laid out in the AASHTO code. The load is comprised of a lane load and semi-truck load. The code recommended lane load of 0.64 klf over a 10 ft. wide traffic lane (AASHTO, p. 3-24). A distribution factor should be applied to this lane load and truck load. The distribution factor is found from the AASHTO code for two or more lanes.

Precast I sections, per AASHTO Table 4.6.2.2.1-1:

$0.075 + \left(\frac{S}{9.5}\right)^{0.6}\left(\frac{S}{L}\right)^{0.2}\left(\frac{K_g}{12.0Lt_s^3}\right)^{0.1}$ (AASHTO Table 4.6.2.2.2b-1),

Open Precast Concrete Boxes, per AASHTO Table 4.6.2.2.1-1:

$\left(\frac{S}{6.3}\right)^{0.6}\left(\frac{Sd}{12.0L^2}\right)^{0.125}$ (AASHTO Table 4.6.2.2.2b-1).

This lane load is combined with the semi-truck tractor trailer combination with an 8 kip front axle load a back axle load of 32 kips spaced 14 feet back and another 32 kip axles loading spaced an additional 14 foot to 30 foot distance depending on maximum load effects (AASHTO, Fig. 3.6.1.2.2-1).

Figure 7 - AASHTO Design Truck (AASHTO LRFD 2012)

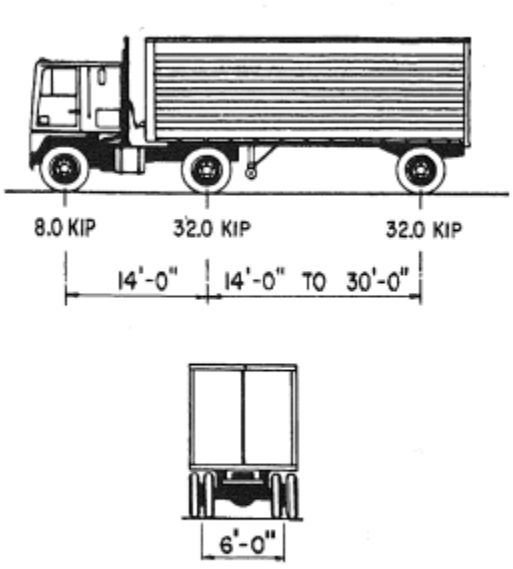

Figure 3.6.1.2.2-1—Characteristics of the Design Truck

To determine the maximum moment induced by this truck, the resultant total load and location must be determined from simple static principles. Once this location is determined, the load is placed on the centerline of the beam half way between the distance from the resultant force and middle axle. The maximum moment occurs at the middle axle load. This can be found using

statics. For design purposes this moment is back calculated to find an equivalent distributed live load. The truck load must be multiplied by a dynamic load allowance (1+IM/100) with IM as per AASHTO Table 3.6.2.1-1.

Table 3.6.2.1-1 – Dynamic Load Allowance, *IM*

Component	IM
Deck Joints-All Limit States	75%
All Other Components: • Fatigues and Fracture Limit State • All Other Limit States	 15% 33%

Table 1

A Multiple Presence factor must also be used for the final load that applies to both lane and truck loads and varies depending on the number of lanes present as per AASHTO Table 3.6.1.1.2-1. The number of lanes is determined by dividing the clear width of the bridge by 12'.

Table 3.6.1.1.2-1 - Multiple Presence Factors, *m*

Number of Loaded Lanes	Multiple Presence Factors, *m*
1	1.20
2	1.00
3	0.85
>3	0.65

Table 2

Load combination and factors vary depending on the calculation for stress and deflection, strength, or fatigue. For stress and deflection calculations the loads are taken as nominal, or simply 1.00DC+1.00LL. However, for calculating tensile stresses in the concrete the Service III combination is used: 1.00DC+0.80LL. For strength, the load combination dead load with live load becomes: 1.25DC + 1.75LL per AASHTO Table 3.4.1-1. Fatigue loads are taken as nominal

with different factors: the truck load is calculated with the distance between 32.0 kip axles is taken as 30.0 feet and the multi-presence factor is shown below:

Table 3.6.1.4.2-1 – Fraction of Truck Traffic in a Single Lane, *p*

Number of Lanes Available to Trucks	*p*
1	1.00
2	0.85
3 or more	0.80

Table 3

The load factor for the fatigue live load is 1.5 (AASHTO Table 3.4.1-1).

After the loads have been applied the stresses must be compared to the code allowed stresses for compliance from ACI 318. Compressive strength limits after strand release at the ends of a simply supported member is $0.70f'_{ci}$, and $0.60f'_{ci}$ elsewhere.

Table 24.5.3.1 – Concrete compressive stress limits immediately after transfer of prestress

Location	Concrete compressive stress limits
End of simply-supported members	$0.70f_{ci}$'
All other locations	$0.60f_{ci}$'

Table 4

Tensile strength limits after strand release at the ends of a simply supported member are $6\sqrt{f'_{ci}}$, and $3\sqrt{f'_{ci}}$, elsewhere.

Table 54.5.3.2 – Concrete tensile stress limits immediately after transfer of prestress, without additional bonded reinforcement in tension zone

Location	Concrete tensile stress limits
End of simply-supported members	$6\sqrt{f'_{ci}}$
All other locations	$3\sqrt{f'_{ci}}$

Table 5

If these tensile limits are exceeded, non-prestressed reinforcing can be added to resist these tensile forces. The mild steel will be added near the top where the tensile forces occur. PCI has a method for calculating the area of steel needed. The height of the compression zone must be calculated:

$c = \frac{f_t}{f_t + f_b}(h)$ (PCI Design Handbook, pp. 5-23).

Next the tensile force is calculated as,

$T = \frac{cf_t b}{2}$ (PCI Design Handbook, pp. 5-23),

then the tension force is divided by the yield strength to calculate the area of steel required $A_{s\,req'd} = \frac{T}{f_y}$. Compressive strength limits at service loads are $0.45f'_{ci}$ for sustained loads and $0.60f'_{ci}$ for total load (excludes Class C members).

Table 24.5.4.1 - Concrete compressive stress limits at service loads

Load Condition	Concrete compressive stress limits
Prestress plus sustained load	$0.45f_c$'
Prestress plus total load	$0.60f_c$'

Table 6

The tensile stress anywhere after release should not exceed $7.5\sqrt{f'_c}$ for Class U members or $12\sqrt{f'_c}$ for Class T members. If the $12\sqrt{f'_c}$ stress limit is exceeded then the member is classified as Class C. Class U is classified as an uncracked section, and the gross section properties can be used for stress calculations and deflection calculations. Class T is classified as the transition between an uncracked section and a cracked section. Deflection calculations for Class T members must use cracked section properties. Class C is a cracked section, therefore all calculations must consider cracked properties.

Table R24.5.2.1 - Serviceability design requirements

	Class U	Class T	Class C
Assumed behavior	Uncracked	Transition between uncracked and cracked	Cracked
Section properties for stress calculations at service loads	Gross section 24.5.2.2	Gross section 24.5.2.2	Cracked section 24.5.2.3
Allowable stress at transfer	24.5.3	24.5.3	24.5.3
Allowable compressive stress based on uncracked section properties	24.5.4	24.5.4	No requirement
Tensile stress at service loads 24.5.2.1	$\leq 7.5\sqrt{f_c'}$	$7.5\sqrt{f_c'} < f_t \leq 12\sqrt{f_c'}$	No requirement
Deflection calculation basis	24.2.3.8, 24.2.4.2 Gross section	24.2.3.9, 24.2.4.2 Cracked section, bilinear	24.2.3.9, 24.2.4.2 Cracked section, bilinear
Crack control	No requirement	No requirement	24.3
Computation of Δf_{ps} or Δf_s for crack control	-	-	Cracked section analysis
Side skin reinforcement	No requirement	No requirement	9.7.2.3

Table 7

The moment capacity of the prestressed beam is calculated the same as a non-prestressed member. The compressive strength of the Whitney stress block is $0.85f_c'$ with a depth of $a = \beta_1 c$. The values of β_1 are found in ACI Table 22.2.2.4.3.

Table 22.2.2.4.3 - Values of β_1 for equivalent rectangular concrete stress distribution

f_c', psi	β_1	
$2500 \leq f_c' \leq 4000$	0.85	(a)
$4000 < f_c' < 8000$	$0.85 - \frac{0.05(f_c' - 4000)}{1000}$	(b)
$f_c' \geq 8000$	0.65	(c)

Table 8

Bridge girders often have a cast-in-place concrete decking that acts compositely with the bridge girder when hardened, and thus should not be ignored. Composite action changes the member's properties dramatically and can help the capacity, lower stresses, and reduce the amount of camber/deflection a member undergoes during the crucial live loading. The compression block will occur in the composite decking in most cases. Strain compatibility should be used to calculate the ultimate bending capacity (just as in ordinary reinforced concrete beams).

If mild steel is needed to achieve strength, it is simply added to the reinforcing strength $A_{ps}f_{ps} + A_s f_Y$. The strength reduction factor is $\Phi = 1.0$. The diagram below shows the application of the nominal flexural resistance principles expressed previously.

Figure 8 - (PCI Design Handbook)

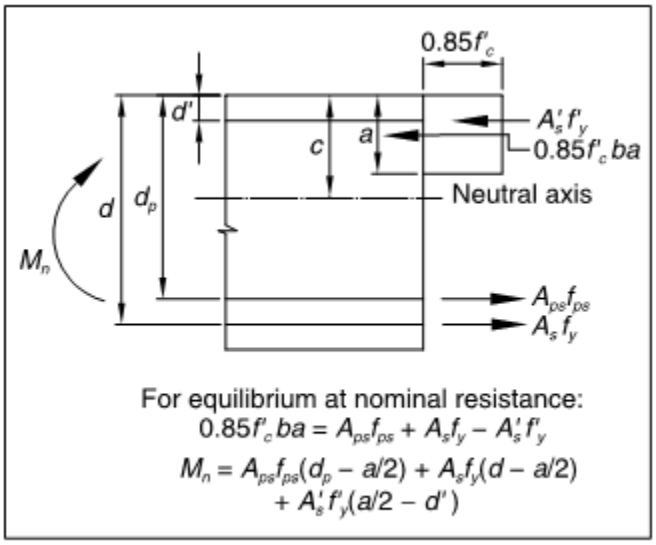

Fig. 5.2.1 Nominal flexural resistance.

The strains associated with the nominal flexural resistance are shown in the figure below.

Figure 9 - (Design of Prestressed Concrete Structures)

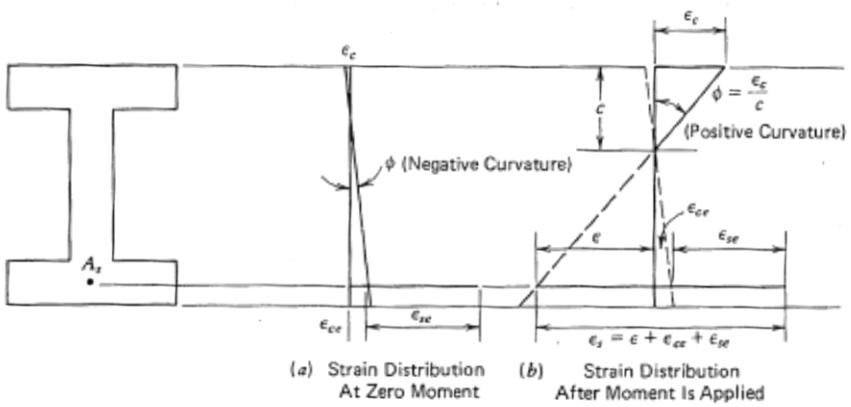

Fig. 5-20. Distribution of strain assumed.

A very complex, but important topic is the idea of prestress losses. The prestress loss calculations are set forth in both the PCI Design Handbook and AASHTO Design Specification. These equations are estimates and will yield similar results. The spreadsheet calculates both the

PCI method and the AASHTO method for losses but uses the AASHTO method for accurate member design. PCI provides guidance to calculate losses due to anchorage seating losses, elastic shortening, creep, shrinkage, and relaxation of tendons. Losses due to anchorage seating and friction occur for posttensioned members and is not included in the loss calculations. Elastic shortening occurs when the prestress strands are released and the concrete shortens. Elastic shortening is the only loss that applies directly after release for pretensioned beams. Shrinkage of the concrete around the prestressing strand reduces the amount of stress in the steel. Creep of the concrete and relaxation of the prestressing stands vary based on the applied forces and duration of load. The initial prestressing stress to ultimate stress ratio of the strands is assumed to 0.75. The total loss can be summarized as

$TL = ES + CR + SH + RE$ (PCI, Eq. 5-63).

The elastic shortening equation is as follows:

$ES = K_{es}E_{ps}f_{cir}/E_{ci}$ (PCI, Eq. 5-64).

Where, K_{es} is 1.0, E_{ps} is 2,8500,000 psi, and E_{ci} is the modulus of elasticity when the prestressing is applied ($33\gamma^{1.5}\sqrt{f_{ci}}$, psi). f_{cir} is the compressive strength of the concrete at the center of gravity of the steel right when the prestress has been applied.

$f_{cir} = K_{cir}\left(\frac{P_i}{A_g} + \frac{P_i e^2}{I_g}\right) - \frac{M_g e}{I_g}$ (PCI, Eq. 5-65).

Where, K_{cir} is 0.9, P_i is the initial prestress force assuming $0.75f_{pu}$ in design examples (lbs), e is the eccentricity of the prestressing stands to the center of gravity to the concrete shape (in), A_g is the gross cross section area of the concrete section (in^2), I_g is the moment of inertia of the gross concrete section (in^4), and M_g is the gravity moment present at the time of prestressing (in-lb). Occasionally, nonprestressed reinforcing is used in load balanced members. The use of mild steel

reduces the amount of strain in the concrete and lowers the amount of elastic shortening losses. This occurrence must be accounted for during design with mild steel. In a similar manner, mild steel also reduces the effects of long term camber and creep. The equation for creep is

$CR = K_{cr}(E_{ps}/E_c)(f_{cir} - f_{cds})$ (PCI, Eq. 5-66).

Where, K_{cir} is 2.0 for normal weight concrete, E_c is the modulus of elasticity of the concrete at 28 days (psi), f_{cds} is the stress in the concrete at the center of gravity of the steel when all sustained dead load is applied

$f_{cds} = M_{sd}(e)/I_g$ (psi) (PCI, Eq. 5-67),

and M_{sd} is the moment due to all sustained dead load (in-lb). The loss attributed to the shrinkage of concrete is

$SH = (8.2 \times 10^{-6})K_{sh}E_{ps}(1 - 0.06V/S)(100 - RH)$ (PCI, Eq. 5-68).

K_{sh} is 1.0 for pretensioned beams, V/S is the volume to surface area ratio, and RH is the average ambient relative humidity taken as 65 for design example. Calculation for the relaxation of the tendons can be calculated by

$RE = [K_{re} - J(SH + CR + ES)]C$ (PCI, Eq. 5-69).

K_{re} is 5000 psi for Grade 270 low-relaxation strands (PCI, Table 5.7.1), J is 0.040 for Grade 270 low-relaxation stands (PCI, Table 5.7.1), and C is 1.00 for $f_{pi}/f_{pu} = 0.75$ and low-relaxation strands (PCI, Table 5.7.2). These losses must be calculated at critical sections along the beam: at the end of the transfer length (60 bar diameters), 0.40L for prestress deflected at midspan only, and at midspan. To determine its adequacy, the losses are then subtracted from the initial strand stress and used to calculate the stresses at the tension and compression fibers of a member.

The AASHTO loss calculations are much more detailed, but are fairly close in total calculated prestress losses. Pretensioned strand loss calculations are attributed to the elastic shortening losses in addition to the total time dependent losses:

$\Delta f_{pT} = \Delta f_{ES} + \Delta f_{pLT}$ (AASHTO Eq. 5.9.5.1-1).

The elastic shortening loss calculation is

$\Delta f_{ES} = \frac{E_p}{E_{ct}} f_{cgp}$ (AASHTO Eq. 5.9.5.2.3a-1).

AASHTO allows an approximate method for calculating total time dependent losses with equation 5.9.5.3-1, however for accuracy the refined estimate of time dependent losses is utilized. The refined method calculates the time dependent losses with the following equation:

$\Delta f_{pLT} = \left(\Delta f_{pSR} + \Delta f_{pCR} + \Delta f_{pR1}\right)id + \left(\Delta f_{pSD} + \Delta f_{pCD} + \Delta f_{pR2} - \Delta f_{pSS}\right)df$ (AASHTO Eq. 5.9.5.4.1-1).

The first half of the equation deals with time dependent losses up to the time of deck placement, while the latter half calculates losses after the time of deck placement. The loss calculation due to the shrinkage for girder shrinkage is found by

$\Delta f_{pSR} = \varepsilon_{bid} E_p K_{id}$ (AASHTO Eq. 5.9.5.4.2a-1).

Where,

$K_{id} = 1/1 + \frac{E_p A_{ps}}{E_{ci} A_g}\left(1 + \frac{A_g e_{pg}^2}{I_g}\right)\left[1 + 0.7\psi_b\left(t_f, t_i\right)\right]$ (AASHTO Eq. 5.9.5.4.2a-2)

and

$\varepsilon_{bid} = k_s k_{hs} k_f k_{td} 0.48 \times 10^{-3}$ (AASHTO Eq. 5.4.2.3.3-1).

Additionally, supporting calculations are expressed as

$\psi_b(t, t_i) = 1.9k_s k_{hc} k_f k_{td} t_i^{-0.118}$ (AASHTO Eq. 5.4.2.3.2-1),

$k_s = 1.45 - 0.13(V/S) \geq 1.0$ (AASHTO Eq. 5.4.2.3.2-2),

$k_{hc} = 1.56 - 0.008H$ (AASHTO Eq. 5.4.2.3.2-3),

$k_f = \frac{5}{1+f'_{ci}}$ (AASHTO Eq. 5.4.2.3.2-4),

$k_{td} = \frac{t}{61-4f'_{ci}+t}$ (AASHTO Eq. 5.4.2.3.2-5),

and

$k_{hs} = 2.00 - 0.014H$ (AASHTO Eq. 5.4.2.3.3-2).

The losses due to the creep of the girder are equated by

$\Delta f_{pCR} = \frac{E_p}{E_{ci}} f_{cgp} \psi_b(t_d, t_i) K_{id}$ (AASHTO Eq. 5.9.5.4.2b-1).

The relaxation of the prestressing strands creates losses found by

$\Delta f_{pR1} = \frac{f_{pt}}{K_L}\left(\frac{f_{pt}}{f_{py}} - 0.55\right)$ (AASHTO Eq. 5.9.5.4.2c-1).

The losses after deck placing are similar to losses before deck placement with the time adjusted accordingly. The shrinkage of the girder after deck placement to final time is calculated as

$\Delta f_{pSD} = \varepsilon_{bdf} E_p K_{df}$ (AASHTO Eq. 5.9.5.4.3a-1)

with

$K_{df} = 1/1 + \frac{E_p A_{ps}}{E_{ci} A_c}\left(1 + \frac{A_c e_{pc}^2}{I_c}\right)\left[1 + 0.7\psi_b(t_f, t_i)\right]$ (AASHTO Eq. 5.9.5.4.3a-2)

and all other factors adjusted for the final time and bridge deck placement. The losses due to the creep of the girder after the slab has been cast are found by

$\Delta f_{pCD} = \frac{E_p}{E_{ci}} f_{cgp}\left[\psi_b(t_f, t_i) - \psi_b(t_d, t_i)\right]K_{df} + \frac{E_p}{E_c}\Delta f_{cd}\psi_b(t_f, t_d)K_{df}$ (AASHTO Eq. 5.9.5.4.3b-1).

The relaxation of the prestressing strands between the time of the deck placement and final time is the same, thus yielding $\Delta f_{pR2} = \Delta f_{pR1}$ (AASHTO Eq. 5.9.5.4.3c-1). The prestress gain from the shrinkage of the deck is determined by

$\Delta f_{pSS} = \frac{E_p}{E_c}\Delta f_{cdf} K_{df}\left[1 + 0.7\psi_b(t_f, t_d)\right]$ (AASHTO Eq. 5.9.5.4.3d-1),

with

$\Delta f_{cdf} = \frac{\varepsilon_{ddf} A_d E_{cd}}{\left[1+0.7\psi_d(t_f,t_d)\right]}\left(\frac{1}{A_c} - \frac{e_{pc}e_d}{I_c}\right)$ (AASHTO Eq. 5.9.5.4.3d-2).

The calculation of shears, moments, and deflections/cambers are all related or found in a similar manner. The externally applied moments along the length of the member can be calculated as

$M_x = \frac{wx}{2}(l - x)$.

Deflection from externally applied forces along the length of a member are found by

$\Delta = \frac{wx}{24EI}(l^3 - 2lx^2 + x^3)$.

Figure 10 - Design Aid 15.1.3 Beam Design Equations and Diagrams (PCI Design Handbook)

1B.1 SIMPLE BEAM – UNIFORMLY DISTRIBUTED LOAD

$R = V$ ..... $= \frac{w\ell}{2}$

V_x ..... $= w\left(\frac{\ell}{2} - x\right)$

M_{max} (at center) ..... $= \frac{w\ell^2}{8}$

M_x ..... $= \frac{wx}{2}(\ell - x)$

Δ_{max} (at center) ..... $= \frac{5w\ell^4}{384EI}$

Δ_x ..... $= \frac{wx}{24EI}(\ell^3 - 2\ell x^2 + x^3)$

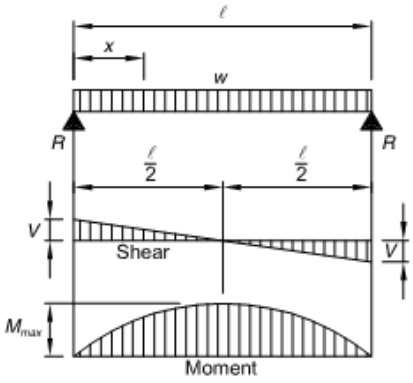

The camber induced from the internal prestressing force of straight strands is based upon the curvature (much like the moment) caused by this force, and eccentricity of the force, and center of gravity of the member. Lin and Burns compiled various strand conditions to calculate camber at the midspan of simply supported beams as shown below.

Figure 11 - (Design of Prestressed Concrete Structures)

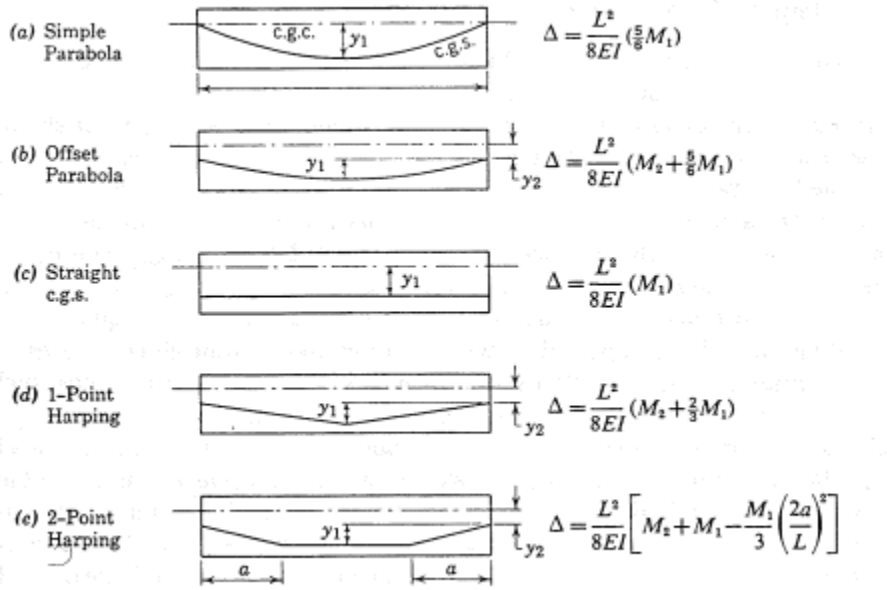

Fig. 8-6. Formulas for computing midspan camber due to prestress (simple beams).

The PCI Design Handbook contains a similar figure with a more information. However, the PCI Handbook does not consider the total effects from some conditions (e.g. a single point drape). Lin and Burns have already considered the effects from the axial component and draped component. If the PCI figures are used multiple camber equations may have to be used to account for the multiple effects, as explained later.

Figure 12 - (PCI Design Handbook)

Design Aid 15.1.4 Camber (Deflection) and Rotation Coefficients for Prestress Force and Loads

PRESTRESS PATTERN	EQUIV. MOMENT OR LOAD	EQUIVALENT LOADING	CAMBER +	END ROTATION +	END ROTATION +
(1)	$M = Pe$		$+\frac{M\ell^2}{16EI}$	$+\frac{M\ell}{3EI}$	$-\frac{M\ell}{6EI}$
(2)	$M = Pe$		$+\frac{M\ell^2}{16EI}$	$+\frac{M\ell}{6EI}$	$-\frac{M\ell}{3EI}$
(3)	$M = Pe$		$+\frac{M\ell^2}{8EI}$	$\frac{M\ell}{2EI}$	$-\frac{M\ell}{2EI}$
(4)	$N = \frac{4Pe'}{\ell}$	N	$+\frac{N\ell^3}{48EI}$	$\frac{N\ell^2}{16EI}$	$-\frac{N\ell^2}{16EI}$
(5)	$N = \frac{Pe'}{b\ell}$		$\frac{b(3-4b^2)N\ell^3}{24EI}$	$\frac{b(1-b)N\ell^2}{2EI}$	$-\frac{b(1-b)N\ell^2}{2EI}$
(6)	$w = \frac{8Pe'}{\ell^2}$	W	$\frac{5w\ell^4}{384EI}$	$\frac{w\ell^3}{24EI}$	$-\frac{w\ell^3}{24EI}$

Note: c.g. = center of gravity

The curvature of the member based on the prestressing is calculated by

$$\Phi = \frac{F_p e}{EI}$$

and the upward camber is found by

$$\Delta = \frac{\Phi l^2}{8}.$$

The curvature of a member with a single point drape is found:

$$\Phi = \frac{F_p e'}{EI},$$

with e' becoming the vertical distance between the eccentricity from the end of the member to the middle of the member. The upward camber is calculated by the following equation:

$$\Delta = \frac{\Phi l^2}{12}.$$

The draped strand camber must be added to the camber due to the force and eccentricity at the end of the member. The combination can be visualized in Figure 6 above. The variability of the prestress loss estimates and concrete property variability causes the deflection and camber to be variable. Beyond the variability of the aforementioned principles the most important are the creep and shrinkage of the concrete prestressing member. As the member ages the creep and shrinkage increase, which must be accounted for in the camber and deflection calculations. This topic is very complex and is widely disputed. However, guidelines have been created by many sources; most prominent is the PCI Design Handbook. The PCI Handbook provides multipliers for camber/deflection at multiple stages of a member's lifespan. The multipliers give a general estimate to various loading for member with and without composite topping. Typical bridge girder will have a composite topping so multipliers should be applied shown in the table below:

Table 5.8.2 Suggested simple span multipliers to be used as a guide in estimating long-term cabers and deflections for typical prestressed components

	Without composite topping	With composite topping
At erection:		
(1) Deflection (downward) component – apply to the elastic deflection due to the component weight at release of prestress	1.85	1.85
(2) Camber (upward) component – apply to the elastic camber due to prestress at the time of release of prestress	1.80	1.80
Final:		
(3) Deflection (downward) component – apply to the elastic deflection due to the component weight at release of prestress	2.70	2.40
(4) Camber (upward) component – apply to the elastic camber due to prestress at the time of release of prestress	2.45	2.20
(5) Deflection (downward) component – apply to the elastic deflection due to superimposed dead load only	3.00	3.00
(6) Deflection (downward) component – apply to the elastic deflection caused by the composite topping	-	2.30

Table 9

Fatigue is an important topic when discussing a member that undergoes cyclic loading such as a bridge. However, a prestressed bride girder is of little concern as long as it remains un-cracked. The continuous change of stress is key for fatigue. The stress ranges vary depending upon the material, number of cycles, and lower/upper stress ranges. The closer the stress is to the allowable material stress, then the less the stress range can vary. Experimental data has been collected in this regard to show the stress ranges and number of cycles, known as S_r – N curves. A simple method is outlined in the "Design of Prestressed Concrete Structure" by Lin and Burns and can be found in the figure below. If the member is cracked then the fatigue of the materials

must be checked for the concrete, prestressing strands, and any mild steel added for load balancing.

Figure 13 - (Design of Prestressed Concrete Structures)

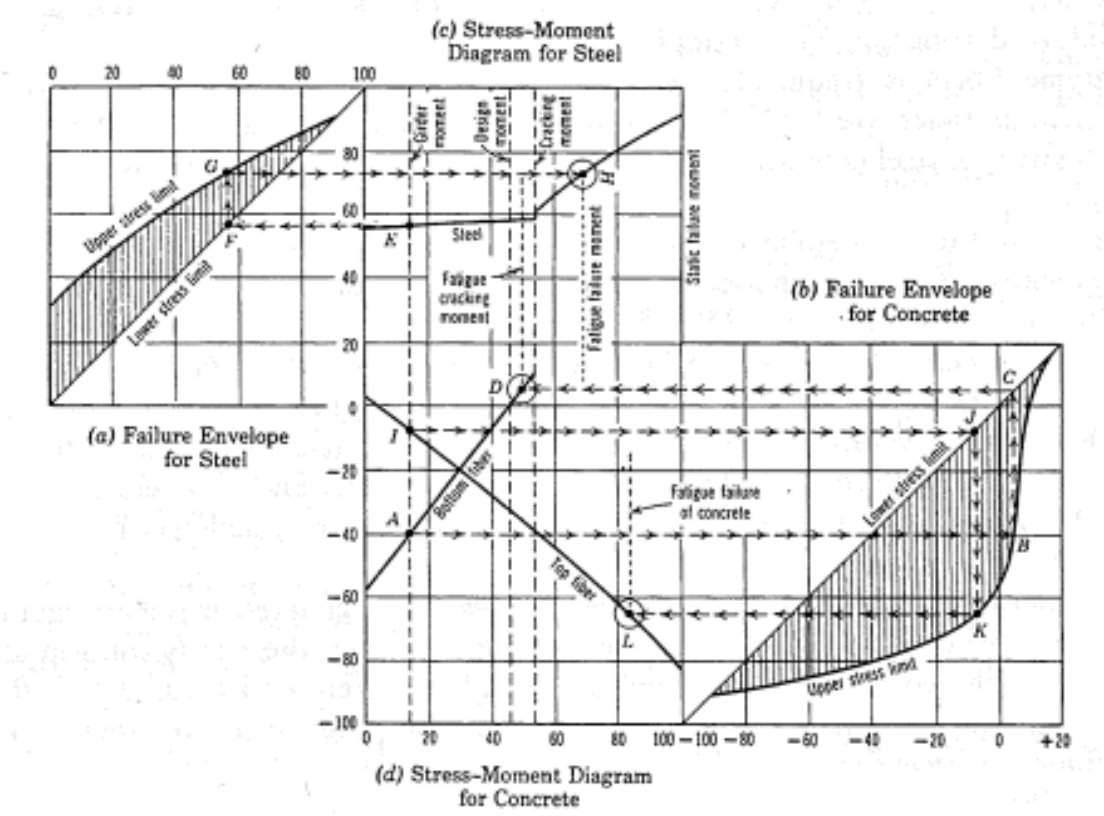

Fig. 2-7. Method for predicting fatigue strength of prestressed concrete beams.

The codified approach is found in the AASHTO code. Fatigue criteria shall meet $\gamma(\Delta f) \leq (\Delta F)_{TH}$ (AASHTO Eq. 5.5.3.1-1). With the value of γ found from Table 3.4.1-1 for Fatigue 1 combination which is 1.5. The limits for the stress change for in reinforcing bars are:

$(\Delta F)_{TH} = 24 - 0.33 f_{min}$ (AASHTO Eq. 5.5.3.2-1).

The limits for the stress change for prestressing strands are 18.0 ksi for radii of curvature in excess of 30', and 10.0 ksi for radii of curvature not exceeding 12' (interpolation is allowed between the two values) per AASHTO Section 5.5.3.3.

Crack width is also very important for serviceability, and durability. If the cracks become extremely wide then the concrete and steel can become debonded, which leads to large stress changes in both materials and could lead to failure. Similarly, cracked sections will lead to higher deflections due to the lower cracked moment of inertia versus the gross moment of inertia. These are very important topics, but durability is of the highest concern for cracking due to chloride infiltration. Chlorides will attack the prestressing strands (which are more vulnerable than mild steel reinforcing) rendering them useless. Cracks width is a concern for bridges because of their close interaction with water, freeze thaw, and deicing chemicals. ACI 224R provides guidance for calculating crack width in reinforced concrete member as follows:

$w = 0.076\beta f_s \sqrt[3]{d_c A} \times 10^{-3}$ (ACI 224R Eq. 1-1).

And a later re-evaluation:

$w = 2\frac{f_s}{E_s}\beta\sqrt{d_c^2 + \left(\frac{s}{2}\right)^2}$ (ACI 224R Eq. 1-2).

However, ACI224R also provides specific crack width calculations for prestressed beams. The committee recognizes that the cracks appear only under transient live load and thus should be controlled for aesthetic reasons. The first set of equations is based on the concrete stress:

$w = C_1 \frac{f_{ct}}{E_c} d_c$ (ACI 224R Eq. 4-17)

and

$w = C_2 \frac{f_{ct}}{E_c} d_c \sqrt[3]{A}$ (ACI 224R Eq. 4-18).

Where C_1=16 and C_2 =12 for strands. Equation 4-17 matched most data, but equation 4-18 proved more accurate with wide beams and larger spacing. The United States Navy uses a method to calculate crack width at the reinforcing bars which can be adjusted by the ratio of the distance

from the neutral axis to the tension face by the distance from the neutral axis to the centroid of reinforcement for crack width at the face. For pretensioned beams the equation is:

$w_{max} = 5.85 \times 10^{-5} \frac{A_t}{\Sigma_o} (\Delta f_s)$ (ACI 224R Eq. 4-19).

Additionally, AASHTO provides a similar equation to calculate reinforcement spacing based upon Class 1 exposure (crack width is 0.017") or Class 2 (varies upon jurisdiction). The spacing shall satisfy

$s \leq \frac{700\gamma_e}{\beta_s f_{ss}} - 2d_c$ (AASHTO Eq. 5.7.3.4-1)

with

$\beta_s = 1 + \frac{d_l}{0.7(h-d_c)}$.

According to PCI Design Handbook a crack width of 0.012 inches or less will not affect the structural integrity, but when exposed to weather the crack should be limited to 0.005 inches. ACI 224R has similar limit states in Table 4.1.

Table 4.1-Guide to reasonable crack widths, reinforced concrete under service loads

Exposure condition	Crack width in.
Dry air or protective membrane	0.016
Humidity, moist air, soil	0.012
Deicing chemicals	0.007
Seawater and seawater spray, wetting and drying	0.006
Water-retaining structures	0.004

Table 10

Most bridges will encounter deicing salts and should be limited to avoid corrosion.

The wide range of information provided in this section was necessary to reveal the background required for future calculations throughout the remaining sections.

CHAPTER III

METHODOLOGY

Several bridge designs were investigated with constrained variables. A comparison of results from these bridge designs form the basis for the thesis and its conclusions. Primarily, a varying amount of load balancing was investigated. The designs' difficulty lies with the application of two dead load components: the bridge girder weight, and a concrete deck that is made composite with cast-in-place concrete. This proves difficult because the slab weight is significant. Most of the load balancing that is performed in buildings resist dead loads that are in place when the tendons are prestressed. The challenge in bridge girders is to balance dead loads that are not yet in place to resist the effects of prestressing.

An outline of the methodology is provided below:

I. AASHTO Type IV Girders were investigated for this thesis. No other cross sections were considered.
II. Following is a list of the variations that were investigated. The "variable" is the amount of dead load that is balanced, or in the case of the DOT design their design methods were employed:
    a. Design from the Oklahoma Department of Transportation (ODOT) for comparison,
    b. Load Balance Design for beam weight only,

c. Load Balance Design for beam weight and ½ of the slab weight,

d. Load Balance Design for beam weight and ¾ of the slab weight, and

e. Load Balance Design for beam weight and total slab weight

III. Following are the material properties that were assumed for computation:

a. Concrete strength = 10,000 psi

b. Concrete release strength = 7,000 psi

c. Concrete Elastic Modulus = 5762 ksi (computed from ACI 318 design equation for modulus)

d. 0.6" diameter, Gr. 270, low relaxation stands

e. Gr. 60 mild steel

A spreadsheet was created to analyze concrete prestressed members. Cross section properties and material properties were entered into the spreadsheet along with load information. Once these values are input, the member was analyzed for compliance with allowable limits and strength. Five AASHTO Type IV bridge girder sections are considered. First, a typical member was designed using basic data provided from ODOT for the Type IV girder. Typical design values from this DOT was used to analyze the girders to find the adequacy of the member, amount of camber/deflection, amount of prestressing used, and the vulnerability to cracking. This design was used as a basis for comparison to the load balancing designs. The four additional load balancing method designs include balancing just the beam weight, balancing the beam weight and 50% of the slab weight, balancing the beam weight and 75% of the slab weight, and finally balancing the beam weight and 100% of the slab weight. The designs were compared to reveal the advantages and disadvantages of the load balancing method for designing prestressed members.

An Excel ® spreadsheet was created for ease of design. A full print out example can be found in the appendix. Material and cross section properties were input into the spreadsheet,

which check the ultimate strength, allowable stresses at the top and bottom of the section over various lengths, and camber/deflections. The adequacy of the member was then calculated. First, the beam and material properties were entered. The beam properties are usually predetermined given a cross section. For example, the bridge girder used for design method comparison is an AASHTO Type IV girder, thus the beams cross section properties have already been tabulated by many sources and were simply entered into the spreadsheet. The transformed section considering the steel was calculated for more accurate results for stresses and deflections. However, the transformed section was ignored for design calculations because the loss calculations utilize gross section properties (as shown in the loss calculation equations). The composite transformed properties with the deck have also been considered for calculations after composite action. These section properties were calculated using simple static principles. The material properties (same as DOT member) were inputted. The Type IV bridge girder section and material properties are shown below:

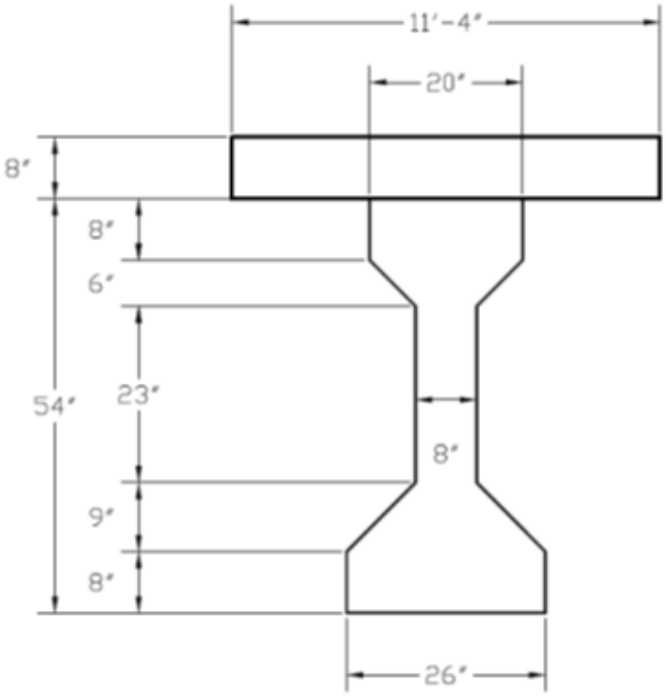

Figure 14-AASHTO Type IV Girder Section

Beam Properties

Area	789.00	in^2
Yt	29.27	in
Yb	24.73	in
I	260730.00	in^4
St	8907.76	in^3
Sb	10543.07	in^3
V/S	4.90	in
Depth	54.00	in
Length	100.00	ft
Slab t	8.00	in
Spacing	11.33	ft

Transformed Properties

838.37	in^2	
30.13	in	
23.87	in	
270690.53	in^4	
8983.44	in^3	
11341.24	in^3	
n	4.95	

Deck Transformed Properties

1518.64	in^2	
21.29	in	
40.71	in	
684221.68	in^4	
32145.35	in^3	
16805.25	in^3	
n	0.67	

Input
Calc.

Material Properties

fps	270.00	ksi
fs	60.00	ksi
fci	7.00	ksi
fc	10.00	ksi
f'c slab	4.50	ksi
Es	29000.00	ksi
Eps	28500.00	ksi
Eci	4820.75	ksi
Ec	5761.90	ksi
Eslab	3865.20	ksi
db	0.60	in^2
Aps	0.22	in^2
β1	0.65	

Next the loads were determined. The dead load was calculated by summing up the self-weight of the materials and any sustained loading on the member. This includes the weight of the member (using normal weight concrete, 150 pcf), weight of the deck, and weight of any additional permanently imposed loads (such as diaphragms, haunches, and railings). The dead load 1 accounts for the haunch from the camber and is applied pre-composite. The dead load 2 account for railing and barriers that is applied post-composite. The dead loads and moments are shown below. The live load is based on the HL 93 loading that includes both a lane load and a

truck load. The HL93 plus the impact is converted to 1.66 klf as shown, and the description of that calculation is in the paragraphs to follow.

Loads

Self	0.822	klf
Slab	1.133	klf
Dead 1	0.150	klf
Dead 2	0.250	klf
Live	1.660	klf

Moments @ Midspan			**Moments @ 60db**	
Self	1027.34	k-ft	119.58	k-ft
Dead 1	1603.75	k-ft	186.68	k-ft
Dead 2	312.50	k-ft	36.38	k-ft
Live	2075.00	k-ft	241.53	k-ft
Md	2943.59	k-ft	342.63	k-ft
Ml	2075.00	k-ft	241.53	k-ft

The live load is any load that can be expected during the member's lifespan. This live load is prescribed by governing design codes. The controlling live load for bridge girders is found in the AASHTO Bridge Design Specifications and is a little more complex due to the variability of traffic loads. This live load is prescribed in the literature review. The truck load parameters were input into the spreadsheet along with any factors to find the maximum design moment. This moment was then equated to a uniform load as shown in the loads above. The calculation of the live load moment is shown:

Truck Live Load Moment

Front Wheel	8.00	k
Mid Wheel	32.00	k
Rear Wheel	32.00	k
Span	100.00	ft
Distance 1-2	14.00	ft
Distance 2-3	14.00	ft
x bar	18.67	ft
Distance to 1	33.67	ft
Reaction L	34.32	k
Moment	1523.92	k-ft
w	1.22	klf
Multi-pres.	1.00	
Lane Load	0.64	klf
Dynamic F	1.33	
Distribution	0.73	
w use	1.66	klf

The detailed live load calculation is explained in the background information.

Another important topic in prestressed concrete is the effective prestressing force after all losses are calculated. The prestress losses are very important to accurately predict because over- or under-predicting the losses can have adverse effects on the member (e.g. excessive deflection or camber, cracking, and miscalculation of stresses at service load conditions). There are various loss calculations from multiple sources, notably AASHTO and PCI. These predictions must include the effects of losses of prestressing during release, elastic shortening of concrete, creep, shrinkage, and relaxation of prestressing strands. PCI provides equations and guidance on all of these loss categories. AASHTO has similar loss equations for prestressed bridge girder design. These two methods are quite different as AASHTO is much more detailed, but the end loss percentage is comparable. The spreadsheet uses the section properties and materials, along with a

few additional factors such as the amount of days during each stage of the prestressed member (time from casting to de-tensioning, deck placement, and final age of design), and relative humidity. An example of the AASHTO loss calculations is shown below:

AASHTO Loss Method (Midspan)					**Supplemental Parameters**		
Δf_{ES}	18.59	ksi	9.18	%	ϵ_{bid}	0.000241	
Approximate					ϵ_{bdf}	0.000324	
Δf_{pLT}	25.54	ksi	12.61	%	ψ_b	0.724532	
					ψ_{bif}	0.972812	
Δf_{pT}	44.13	ksi	21.79	%	ψ_{bdf}	0.972584	
Refined					K_{id}	0.843282	
Before Deck					K_{bdf}	0.91208	
Δf_{pSR}	5.80	ksi	2.86	%	ti	7	days
Δf_{pCR}	11.36	ksi	5.61	%	td	100	days
Δf_{pR1}	1.27	ksi	0.63	%	tf	3650	days
Δf_{pdT}	18.42	ksi	9.10	%	RH	65	%
After Deck					Δf_{cgp}	3.143689	
Δf_{pR2}	1.27	ksi	0.63	%	Δf_{cgpd}	1.67881	
Δf_{pSD}	8.42	ksi	4.16	%	ε_{ddf}	0.00047	
Δf_{pCD}	0.00	ksi	0.00	%	Δf_{cdf}	0.339279	
Δf_{pSS}	2.57	ksi	1.27	%	(V/S)d	4	
Δf_{pLT}	30.69	ksi	15.15	%			
Δf_{pT}	49.27	ksi	24.33	%			

The detailed explanation of both the PCI and AASHTO loss calculations are found in the back ground information. The loss calculations from the AASHTO design code should be used in lieu of the PCI loss calculations to achieve the most detailed prestress losses of bridge girders. These losses must be subtracted from the specified strand stress.

To obtain a preliminary design for the load balancing examples, a number of strands and estimate of steel stress after all losses were input, to obtain an eccentricity. This allows the user to obtain a design that is practical (the number of strands must give a reasonable eccentricity). The calculation utilizes the basis of load balancing, $M_d = F_p \times e$. An example is shown below:

Load Balancing Method

ws	0.822	klf
wd	1.125	klf
L	100	ft
Ase	0.217	in^2
fse	150	ksi
yb	24.73	in

Load Balance Method 1

Beam Only

n	20	
e	18.94	in
g	5.79	in

Load Balance Method 2

Beam+0.5*Slab

n	32	
e	19.94	in
g	4.79	in

Load Balance Method 3

Beam+1.0*Slab

n	44	
e	20.39	in
g	4.34	in

This provides a basis for design and the number of strands are located in such a manner to match "g" or the distance from the prestressing center of gravity to the bottom of the member, as shown below.

Strand Location Calculation

Strands		Inches from bottom		
10	@	2	=	20
10	@	4	=	40
10	@	6	=	60
2	@	32	=	64

Σ	32	Σ	184	in^2
		g	5.75	in

Now, this information was used to analyze the beam. This is where the number of strands and eccentricity can be altered. The design input for strands and eccentricity appears as follows:

Try	32.00	strands
g	5.75	in
e	18.98	in
e@60db	18.98	in

The stresses calculated were found from beam mechanics as discussed earlier. These stresses were then checked for code compliance at predetermined locations. The stress limits are outlined in the background information. The number of strands and eccentricity can be adjusted to balance the dead load desired. An example of the stress output is shown below.

Total Stresses @ Midspan

fse	159.21	ksi	
Fse	1105.55	k	
fp/A	-1.40		
fpe/Sb	-1.99		
M1/Sb	2.99		
M2/S'b	0.22		
Ml/S'b	1.19		
fb	1.01	ksi	not okay
fpe/St	2.36		
M1/St	-3.54		
M2/S't	-0.07		
Ml/S't	-0.48		
ft(sust)	-2.66	ksi	okay
ft(tot)	-3.15	ksi	okay

Release Stresses @ Midspan

fse	187.42	ksi	
Fse	1301.47	k	
ft	-0.26	ksi	okay
fb	-2.82	ksi	okay

Release Stesses @ 60 db

fse	183.19	ksi	
Fse	1272.10	k	
ft	0.94	ksi	not okay
fb	-3.77	ksi	okay

Total Stresses @ 60db

fse	152.34	ksi	
Fse	1057.84	k	
fb(sust)	-2.87	ksi	okay
fb(tot)	-2.73	ksi	okay
ft	0.44	ksi	okay

If any of the compressive stresses or tensile stresses are exceeded (shown in red and "not okay"), many options exist to lower the stresses or resist the additional stresses. Draping the strands can lower the stresses (by varying the eccentricity over the length of the member), adding more mild reinforcing steel in areas of high tension (counteracting the high tensile stresses), and debonding/shielding a small percentage of the strands at the end of a member (lowering compressive or tensile stresses imparted on the member by reducing the prestressing force at the ends). Draping (or harping) involves a single point drape configuration near midspan for a simple span member to accomplish a max eccentricity at midspan and the lowest near the ends. The ideal configuration would be parabolic, but this is difficult to achieve. Draped strands are not preferred for precast members and is not considered. Debonding the strands near the ends can have the same effect as draping because of the eccentricity is lowered over the debonding distance. The new eccentricity created from debonding was input and checked for compliance. Bonded reinforcing was also added to counteract any tensile stresses, as discussed previously. If the stresses needed to be lowered, a new number of strands and eccentricity were considered:

Debonding

Try	30.00	strands	
e	16.00	in	
ES	19.31	ksi	
fse	183.19	ksi	
Fse	1192.60	k	
ft	0.47	ksi	okay
fb	-3.19	ksi	okay
x	3.00	ft	okay

Bonded Reinforcement Req'd

c	6.94	in
T	32.57	k
As req'd	0.54	in^2

After the stresses were checked the design must be checked for ultimate strength. The ultimate load capacity is found the same way as non-prestressed concrete members; using the Whitney stress block, the yield strength of non-prestressed reinforcement, and a calculated stress of prestressing strands, f_{ps} . Strain compatibility must be used to determine the prestressing force. If the prestressing strands do not provide enough resistance mild steel can be added. Calculations can be seen in the background.

Ultimate Capacity

dp	57.25	in	
fps	270.00	ksi	
a	4.28	in	
ϕMn	11709.00	k-ft	okay

Serviceability checks were also provided, such as camber, deflection, fatigue, and crack widths. Emphasis was placed on the camber and deflection. There is no guidance in AASHTO for limiting dead load deflection, but ACI allows Span/240 for total floor deflections in which nothing will be damaged by such deflection. The system live load deflection should be limited to Span/800 (AASHTO 2.5.2.6.2). The live load deflection is much more important because once the dead load is applied it will not change. Camber and deflection calculations can be found previously. The PCI method was used for long-term camber and deflections. Output is shown as:

PCI Method

	Non-cracked	
Initial Camber	2.07	in
Initial Deflection	-1.47	in
Initial Total	0.60	in
Camber @ Erection	3.72	in
Deflection @ Erection	-2.72	in
Subtotal @ Erection	1.00	in
Deflection Slab	-1.70	in
Deflection Dead 1	-0.22	in
Deflection Dead 2	-0.14	in
Total @ Erection	-1.06	in
Camber System	4.55	in
Delfection System	-8.54	in
Total System	-3.99	in
Deflection Live	-0.95	in
Total	-4.93	in

+ upward

Dead	l/240	5.00	in
Live	l/800	1.50	in

Fatigue and crack width calculations were provided as discussed earlier, but most bridge girders never experience loads that exceed the cracking moment and thus neither are of concern.

Crack Width (ACI 224R)

w	0.011	in	okay

Spacing (AASHTO)

s	155.75	in	okay
βs	2.43		

Fatigue

γ(Δfps)	0.54	ksi	
ΔFth	18.00	ksi	okay

The methods and calculations explained above were implemented in the spreadsheet determining the member's adequacy. The various bridge girder designs (ODOT and load balancing) are compared in the following section, determining the advantages of designing a member by the load balancing method.

CHAPTER IV

PRESENTATION OF RESULTS

The load balancing methodologies implemented into the design of prestressed members create efficient members that can meet modern code requirements while mitigating serviceability concerns associated with typical modern designs. Most modern designs ignore the benefits of load balancing and solely focus on stress and strength. The Type IV girder DOT/load balancing designs are compared to reveal the advantages and disadvantages of each method.

The design considers a typical bridge girder design for a long span AASHTO Type IV girder. Five girder designs are considered for comparison. First, a girder from the Oklahoma Department of Transportation is analyzed. Then four load balancing designs are considered:

1) Balance beam weight only,
2) Balance beam weight and 50% of slab weight,
3) Balance beam weight and 75% of slab weight, and
4) Balance beam weight and 100% of slab weight.

A typical AASHTO Type IV girder is shown below.

Figure 15-AASHTO Type IV Girder

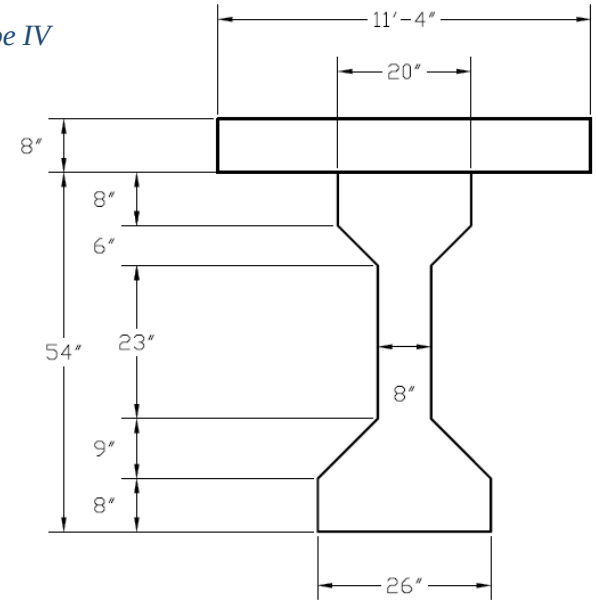

The Type IV bridge design parameters are as follows:

Beam Properties		
Area	789.00	in^2
Yt	29.27	in
Yb	24.73	in
I	260730.00	in^4
St	8907.76	in^3
Sb	10543.07	in^3
V/S	4.90	in
Depth	54.00	in
Length	100.00	ft
Slab t	8.00	in
Spacing	11.33	ft

Deck Transformed Properties		
	1518.64	in^2
	21.29	in
	40.71	in
	684221.68	in^4
	32145.35	in^3
	16805.25	in^3
n	0.67	

Material Properties

fps	270.00	ksi
fs	60.00	ksi
fci	7.00	ksi
fc	10.00	ksi
f'c slab	4.50	ksi
Es	29000.00	ksi
Eps	28500.00	ksi
Eci	4820.75	ksi
Ec	5761.90	ksi
Eslab	3865.20	ksi
db	0.60	in^2
Aps	0.22	in^2
β1	0.65	

Precomposite

Mcr	2948.24	k-ft
Icr**	146143.74	in^4
Ieff	260730.00	in^4

Composite

4634.92	k-ft
164297.41	in^4
573860.14	in^4

**AASHTO Type IV only

Loads

Self	0.822	klf
Slab	1.133	klf
Dead 1	0.150	klf
Dead 2	0.250	klf
Live	1.660	klf

Moments @ Midspan

Self	1027.34	k-ft
Dead 1	1603.75	k-ft
Dead 2	312.50	k-ft
Live	2075.00	k-ft
Md	2943.59	k-ft
Ml	2075.00	k-ft

Moments @ 60db

119.58	k-ft
186.68	k-ft
36.38	k-ft
241.53	k-ft
342.63	k-ft
241.53	k-ft

Ma	5018.59	k-ft
Mu	7310.74	k-ft

584.16 k-ft

The ODOT Type IV design input and output:

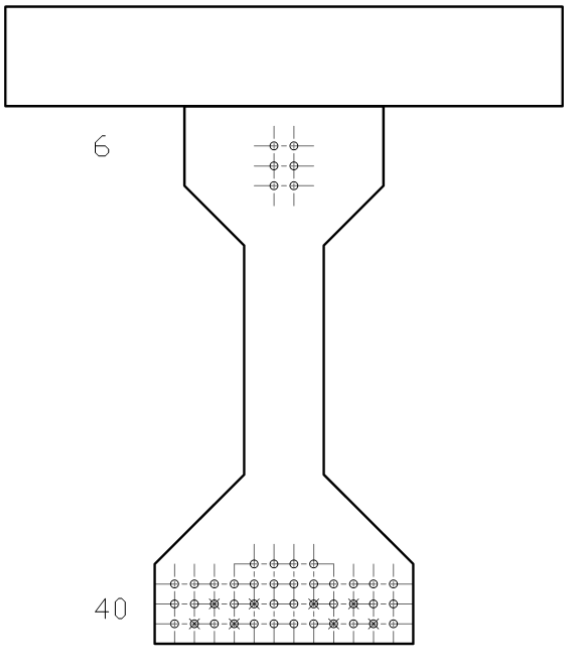

Figure 16-ODOT Type IV

Strand Location Calculation

Strands		Inches from bottom		
12	@	2	=	24
12	@	4	=	48
12	@	6	=	72
4	@	8	=	32
2	@	46	=	92
2	@	48	=	96
2	@	50	=	100
0	@	52	=	0

Σ	46	Σ	464	in^2
		g	10.09	in

The results are shown here:

Try	46.00	strands
g	10.09	in
e	14.64	in
e@60db	14.64	in

Total Stresses @ Midspan

fse	153.23	ksi	
Fse	1529.52	k	
fp/A	-1.94		
fpe/Sb	-2.12		
M1/Sb	2.99		
M2/S'b	0.22		
Ml/S'b	1.19		
fb	0.34	ksi	okay
fpe/St	2.51		
M1/St	-3.54		
M2/S't	-0.07		
Ml/S't	-0.48		
ft(sust)	-3.04	ksi	okay
ft(tot)	-3.53	ksi	okay

Total Stresses @ 60db

fse	148.00	ksi	
Fse	1477.37	k	
fb(sust)	-3.55	ksi	okay
fb(tot)	-3.41	ksi	okay
ft	0.08	ksi	okay

Crack Width (ACI 224R)

w	0.002	in	okay

Spacing (AASHTO)

s	841.32	in	okay
βs	2.43		

Release Stresses @ Midspan

fse	183.91	ksi	
Fse	1835.84	k	
ft	-0.69	ksi	okay
fb	-3.71	ksi	okay

Release Stesses @ 60 db

fse	180.70	ksi	
Fse	1803.70	k	
ft	0.52	ksi	not okay,>6sqrt(f'ci)
fb	-4.65	ksi	okay

Debonding

Try	38.00	strands	
e	13.15	in	
ES	21.80	ksi	
fse	180.70	ksi	
Fse	1490.02	k	
ft	0.15	ksi	okay
fb	-3.61	ksi	okay
x	4.00	ft	okay

Fatigue

γ(Δfps)	0.54	ksi	
ΔFth	18.00	ksi	okay

Ultimate Capacity

dp	57.25	in	
fps	270.00	ksi	
a	4.28	in	
ϕMn	11709.00	k-ft	okay

The stress diagrams at midspan are as follows:

Figure 17-Type IV, ODOT Design Standard midspan stresses at service

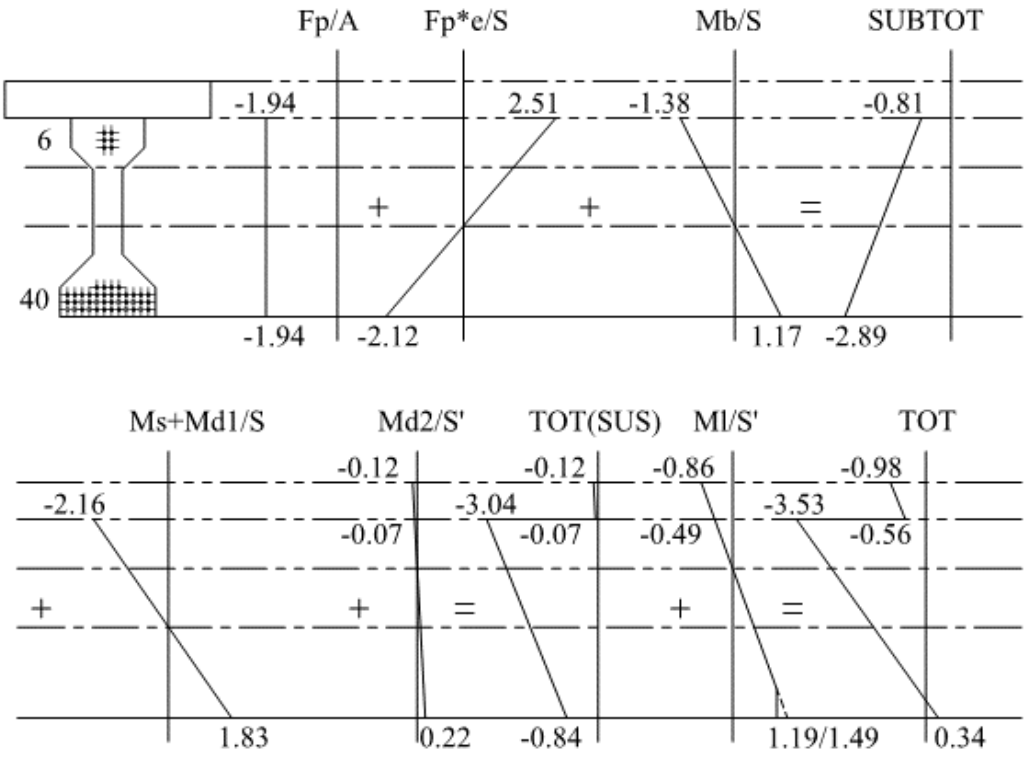

Figure 18-Type IV, ODOT Design Standard release stresses at 60db from the ends (a) without debonding and (b) with debonding.

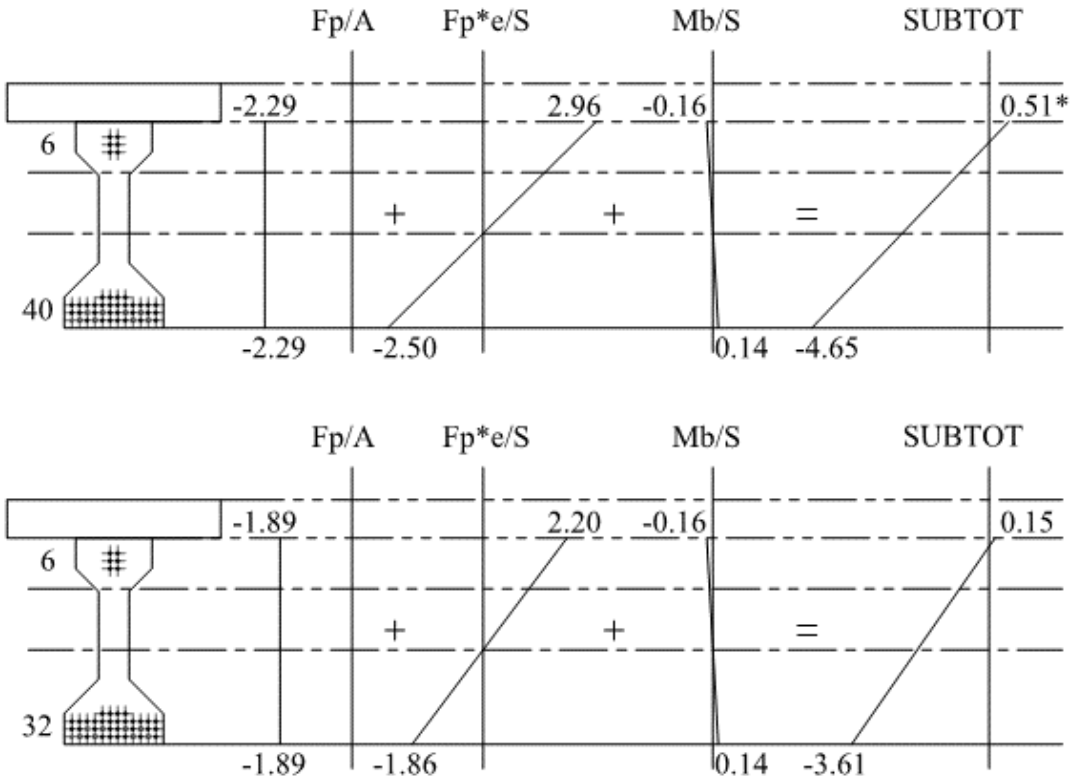

The initial release stresses are shown above and the debonding stresses are shown below the initial stresses. The stresses not meeting codified values are shown with an asterisks. Debonding was required to lower release stresses at the ends, 8 strands at a minimum of 4 ft.

Camber and deflections for the ODOT Design Standard are shown below:

PCI Method

	Non-cracked	
Initial Camber	3.71	in
Initial Deflection	-1.42	in
Initial Total	2.29	in
Camber @ Erection	6.67	in
Deflection @ Erection	-2.62	in
Subtotal @ Erection	4.05	in
Deflection Slab	-1.63	in
Deflection Dead 1	-0.22	in
Deflection Dead 2	-0.14	in
Total @ Erection	2.06	in
Camber System	8.16	in
Delfection System	-8.24	in
Total System	-0.08	in
Deflection Live	-0.95	in
Total	-1.03	in

+ upward

Dead	l/250	4.80	in
Live	l/800	1.50	in

Load Balancing Type IV, beam weight only:

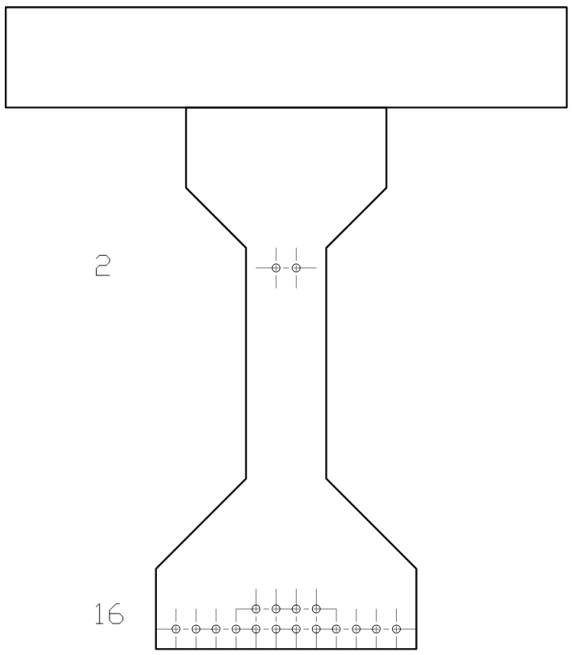

Figure 19-Type IV, beam weight only

Strand Location Calculation

Strands		Inches from bottom		
12	@	2	=	24
4	@	4	=	16
2	@	38	=	76

Σ	18	Σ	116	in^2
		g	6.44	in

The results are as follows:

N	37.47	strands
Try	18.00	strands
g	6.44	in
e	18.29	in
e@60db	18.29	in

Total Stresses @ Midspan

fse	171.43	ksi	
Fse	669.61	k	
fp/A	-0.85		
fpe/Sb	-1.16		
M1/Sb	2.99		
M2/S'b	0.22		
Ml/S'b	1.19		
fb	2.39	ksi	not okay,
fpe/St	1.37		>7.5sqrt(f'c)
M1/St	-3.54		
M2/S't	-0.07		
Ml/S't	-0.48		
ft(sust)	-3.09	ksi	okay
ft(tot)	-3.57	ksi	okay

Release Stresses @ Midspan

fse	196.07	ksi	
Fse	765.83	k	
ft	-0.78	ksi	okay
fb	-1.13	ksi	okay

Release Stesses @ 60 db

fse	191.80	ksi	
Fse	749.17	k	
ft	0.43	ksi	okay
fb	-2.11	ksi	okay

Total Stresses @ 60db

fse	164.46	ksi	
Fse	642.36	k	
fb(sust)	-1.55	ksi	okay
fb(tot)	-1.42	ksi	okay
ft	0.03	ksi	okay

Crack Width (ACI 224R)

w	0.015	in	okay

Spacing (AASHTO)

s	115.86	in	okay
βs	2.43		

Fatigue

γ(Δfps)	0.54	ksi	
ΔFth	18.00	ksi	okay

Ultimate Capacity

dp	58.00	in	
fps	270.00	ksi	
a	2.72	in	
ϕMn	7620.08	k-ft	okay

The stress diagrams at midspan are as follows:

Figure 20-Type IV, beam weight only midspan stresses at service

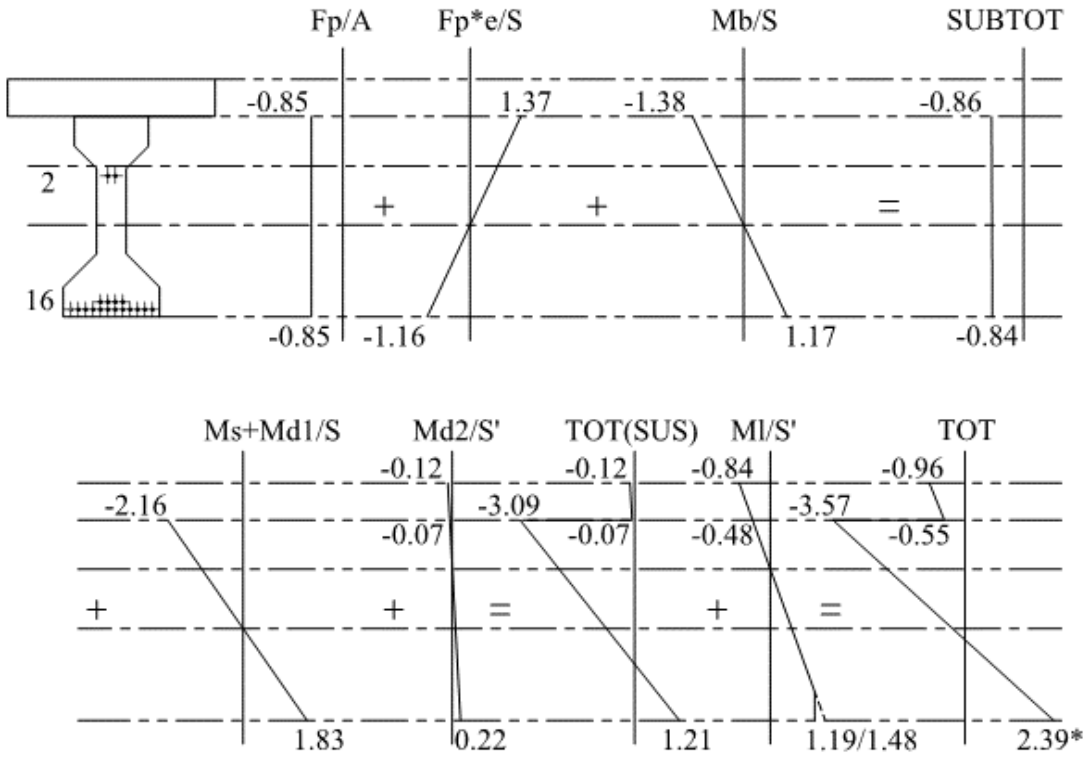

Figure 21-Type IV, beam weight only release stresses at 60db from ends

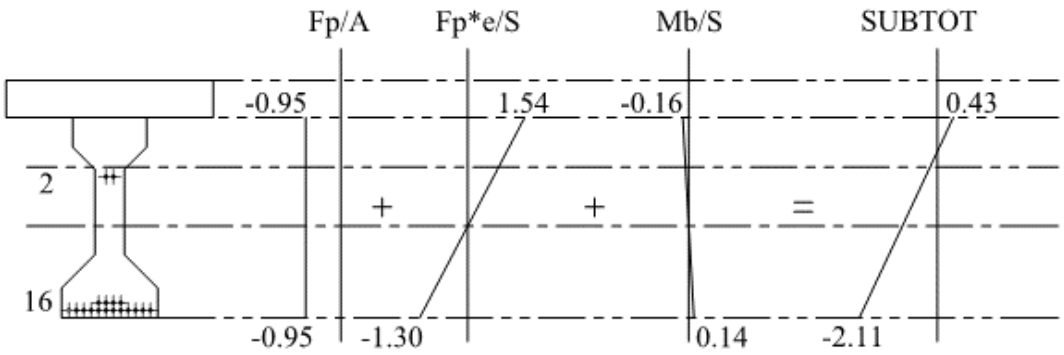

Six #9 reinforcing bars were added at the bottom to increase ultimate strength. No debonding is required.

Camber and deflections are shown below:

PCI Method

	Non-cracked	
Initial Camber	2.01	in
Initial Deflection	-1.47	in
Initial Total	0.53	in
Camber @ Erection	3.61	in
Deflection @ Erection	-2.72	in
Subtotal @ Erection	0.89	in
Deflection Slab	-1.70	in
Deflection Dead 1	-0.22	in
Deflection Dead 2	-0.14	in
Total @ Erection	-1.18	in
Camber System	4.41	in
Delfection System	-8.54	in
Total System	-4.12	in
Deflection Live	-0.95	in
Total	-5.07	in

+ upward

Dead	l/240	5.00	in
Live	l/800	1.50	in

Load Balancing Type IV, Beam weight and 50% slab weight:

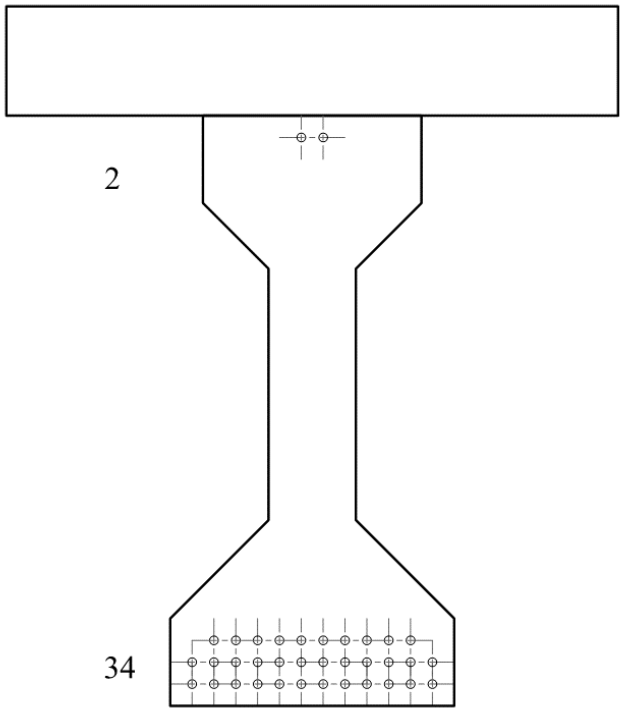

Figure 22-Type IV, beam weight and 50% slab weight

Strand Location Calculation

Strands		Inches from bottom		
12	@	2	=	24
12	@	4	=	48
10	@	6	=	60
2	@	52	=	104

Σ	36	Σ	236	in^2
		g	6.56	in

The results are as follows:

Try	36.00	strands
g	6.56	in
e	18.17	in
e@60db	18.17	in

Total Stresses @ Midspan

fse	156.79	ksi	
Fse	1224.83	k	
fp/A	-1.55		
fpe/Sb	-2.11		
M1/Sb	2.99		
M2/S'b	0.22		
Ml/S'b	1.19		
fb	0.74	ksi	okay
fpe/St	2.50		
M1/St	-3.54		
M2/S't	-0.07		
Ml/S't	-0.48		
ft(sust)	-2.67	ksi	okay
ft(tot)	-3.15	ksi	okay

Release Stresses @ Midspan

fse	185.83	ksi	
Fse	1451.73	k	
ft	-0.26	ksi	okay
fb	-3.17	ksi	okay

Release Stesses @ 60 db

fse	181.82	ksi	
Fse	1420.35	k	
ft	0.94	ksi	not okay,>6sqrt(f'ci)
fb	-4.11	ksi	okay

Total Stresses @ 60db

fse	150.26	ksi	
Fse	1173.86	k	
fb(sust)	-3.14	ksi	okay
fb(tot)	-3.00	ksi	okay
ft	0.43	ksi	okay

Bonded Reinforcement Req'd

c	10.01	in
T	93.71	k
As req'd	1.56	in^2

Crack Width (ACI 224R)

w	0.005	in	okay

Spacing (AASHTO)

s	384.95	in	okay
βs	2.43		

Fatigue

γ(Δfps)	0.54	ksi	
ΔFth	18.00	ksi	okay

Ultimate Capacity

dp	58.00	in
fps	270.00	ksi
a	4.06	in
ϕMn	11244.37	k-ft

okay

The stress diagrams at midspan are as follows:

Figure 23-Type IV, beam weight and 50% slab weight midspan stresses at service

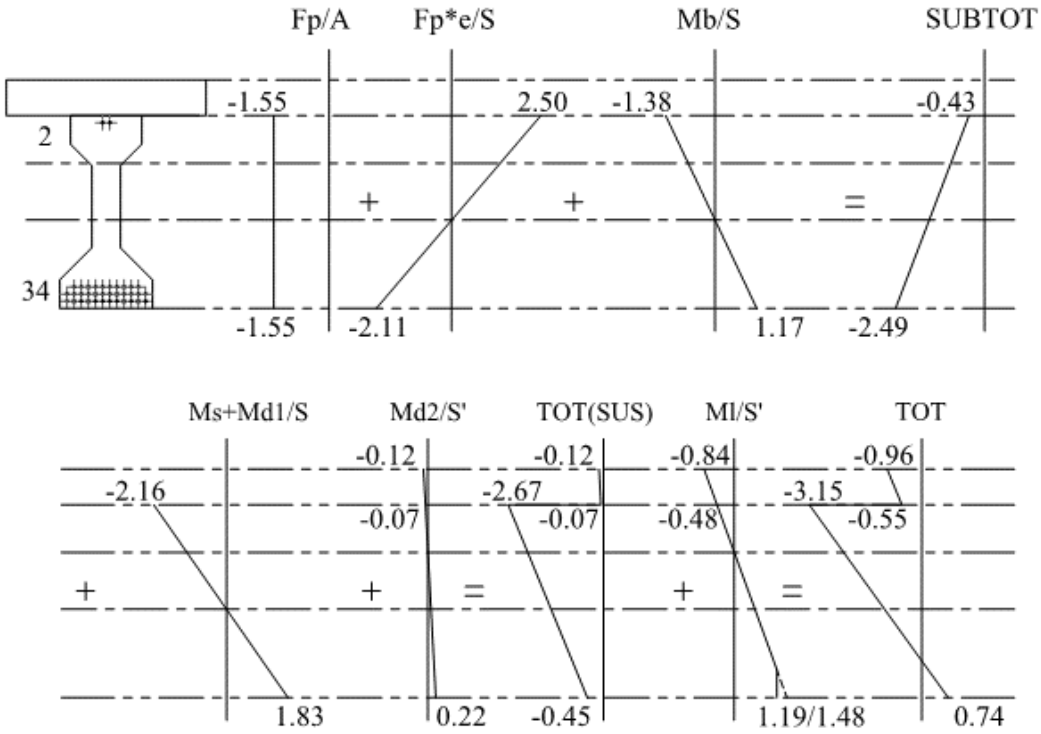

Figure 24-Type IV, beam weight and 50% slab weight release stresses at 60db from ends

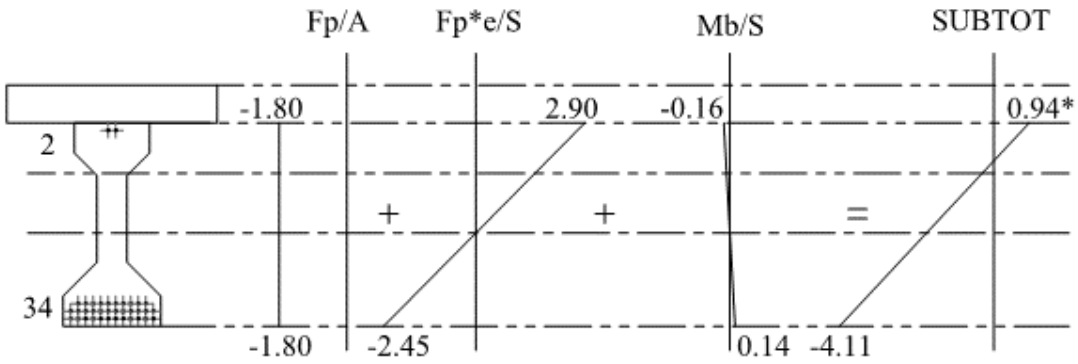

No debonding is required, mild steel is added to the top of the cross section to control cracking caused by tensile stresses at release (2-#9 bars).

Camber and deflections are shown below:

PCI Method

	Non-cracked	
Initial Camber	3.78	in
Initial Deflection	-1.47	in
Initial Total	2.31	in
Camber @ Erection	6.80	in
Deflection @ Erection	-2.72	in
Subtotal @ Erection	4.08	in
Deflection Slab	-1.70	in
Deflection Dead 1	-0.22	in
Deflection Dead 2	-0.14	in
Total @ Erection	2.01	in
Camber System	8.31	in
Delfection System	-8.54	in
Total System	-0.23	in
Deflection Live	-0.95	in
Total	-1.17	in

+ upward

Dead	l/240	5.00	in
Live	l/800	1.50	in

Load Balancing Type IV, Beam weight and 75% slab weight:

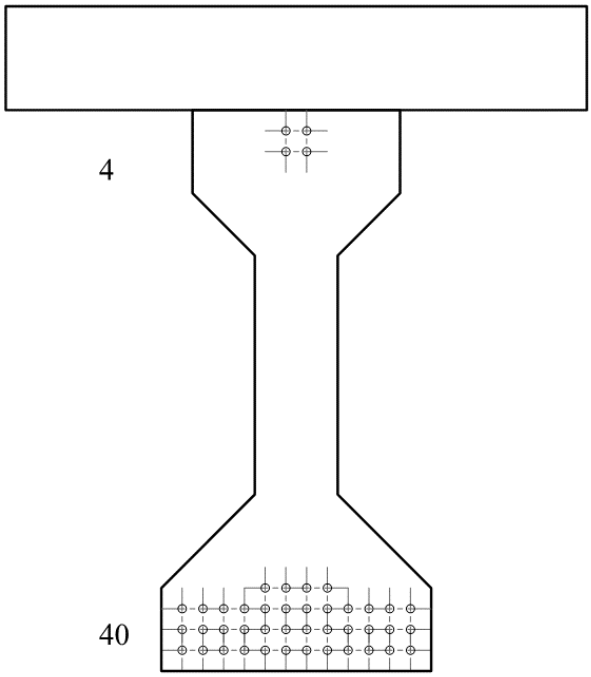

Figure 25-Type IV, beam weight and 75% slab weight

Stand Location Calculation

Strands		Inches from bottom		
12	@	2	=	24
12	@	4	=	48
12	@	6	=	72
4	@	8	=	32
2	@	50	=	100
2	@	52	=	104

Σ	44	Σ	380	in^2
		g	8.64	in

The bottom strands balance the dead load, but top strands were added to reduce debonding and reduce tensile stresses at the top of the cross section.

The results are as follows:

Try	44.00	strands
g	8.64	in
e	16.09	in
e@60db	16.09	in

Total Stresses @ Midspan

fse	153.14	ksi	
Fse	1462.21	k	
fp/A	-1.85		
fpe/Sb	-2.23		
M1/Sb	2.99		
M2/S'b	0.22		
Ml/S'b	1.19		
fb	0.32	ksi	okay
fpe/St	2.64		
M1/St	-3.54		
M2/S't	-0.07		
Ml/S't	-0.48		
ft(sust)	-2.83	ksi	okay
ft(tot)	-3.31	ksi	okay

Release Stresses @ Midspan

fse	183.58	ksi	
Fse	1752.78	k	
ft	-0.44	ksi	okay
fb	-3.73	ksi	okay

Release Stesses @ 60 db

fse	180.05	ksi	
Fse	1719.12	k	
ft	0.77	ksi	not okay,>6sqrt(f'ci)
fb	-4.67	ksi	okay

Total Stresses @ 60db

fse	147.43	ksi	
Fse	1407.62	k	
fb(sust)	-3.56	ksi	okay
fb(tot)	-3.42	ksi	okay
ft	0.28	ksi	okay

Bonded Reinforcement Req'd

c	7.61	in
T	58.22	k
As req'd	0.97	in^2

Crack Width (ACI 224R)

w	0.002	in	okay

Spacing (AASHTO)

s	900.58	in	okay
βs	2.43		

Fatigue

γ(Δfps)	0.54	ksi	
ΔFth	18.00	ksi	okay

Ultimate Capacity

dp	58.00	in
fps	270.00	ksi
a	4.51	in
ϕMn	12449.74	k-ft

okay

The stress diagrams at midspan are as follows:

Figure 26-Type IV, beam weight and 75% slab weight midspan stresses at service

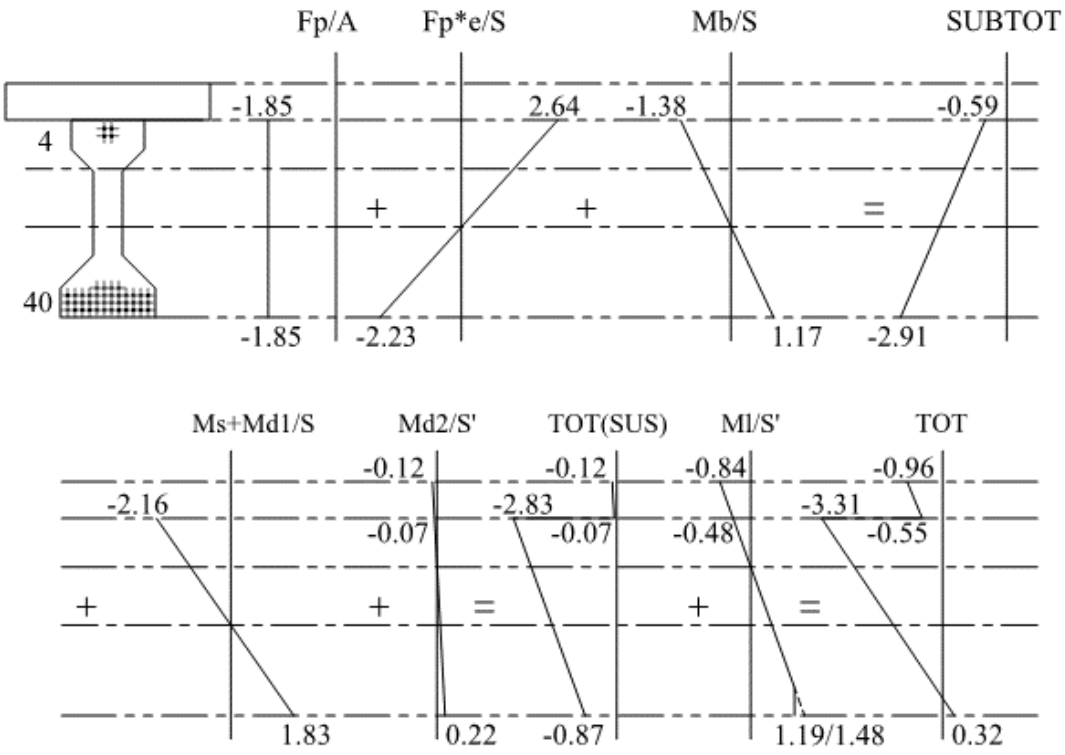

Figure 27-Type IV, beam weight and 75% slab weight release stresses at 60db from ends

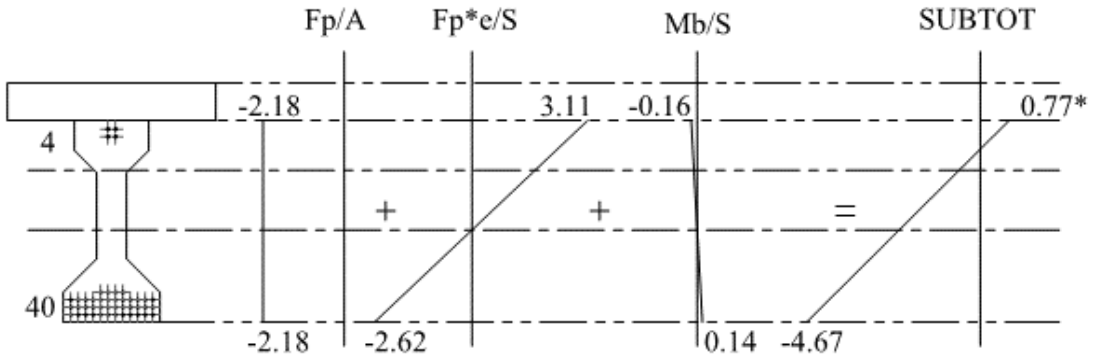

No debonding is required, mild steel is added to the top of the cross section to control cracking caused by tensile stresses at release (1-#9 bar).

Camber and deflections are shown below:

PCI Method

	Non-cracked	
Initial Camber	4.04	in
Initial Deflection	-1.47	in
Initial Total	2.57	in
Camber @ Erection	7.27	in
Deflection @ Erection	-2.72	in
Subtotal @ Erection	4.55	in
Deflection Slab	-1.70	in
Deflection Dead 1	-0.22	in
Deflection Dead 2	-0.14	in
Total @ Erection	2.48	in
Camber System	8.89	in
Delfection System	-8.54	in
Total System	0.35	in
Deflection Live	-0.95	in
Total	-0.60	in

+ upward

Dead	l/240	5.00	in
Live	l/800	1.50	in

Load Balancing Type IV, Beam weight and 100% slab weight:

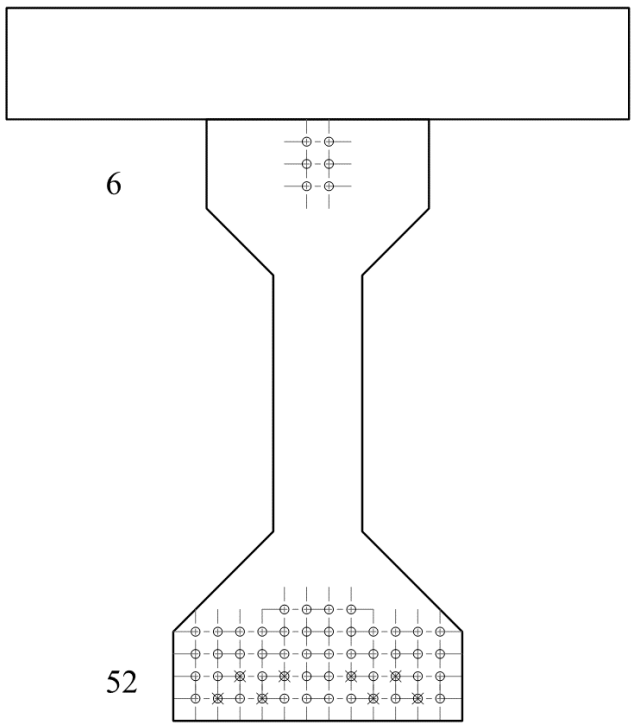

Figure 28-Type IV, beam weight and slab weight

Stand Location Calculation

Strands		Inches from bottom		
12	@	2	=	24
12	@	4	=	48
12	@	6	=	72
12	@	8	=	96
4	@	10	=	40
2	@	48	=	96
2	@	50	=	100
2	@	52	=	104

Σ	58	Σ	580	in^2
		g	10.00	in

The bottom strands balance the dead load, but top strands were added to reduce debonding and reduce tensile stresses at the top of the cross section.

The results are as follows:

Try	58.00	strands
g	10.00	in
e	14.73	in
e@60db	14.73	in

Total Stresses @ Midspan

fse	146.24	ksi	
Fse	1840.61	k	
fp/A	-2.33		
fpe/Sb	-2.57		
M1/Sb	2.99		
M2/S'b	0.22		
Ml/S'b	1.19		
fb	-0.50	ksi	okay
fpe/St	3.04		
M1/St	-3.54		
M2/S't	-0.07		
Ml/S't	-0.48		
ft(sust)	-2.91	ksi	okay
ft(tot)	-3.39	ksi	okay

Total Stresses @ 60db

fse	141.15	ksi	
Fse	1776.55	k	
fb(sust)	-4.36	ksi	okay
fb(tot)	-4.22	ksi	okay
ft	0.21	ksi	okay

Crack Width (ACI 224R)

w	-0.014	in	okay

Spacing (AASHTO)

s	-579.66	in	okay
βs	2.43		

Release Stresses @ Midspan

fse	178.70	ksi	
Fse	2249.12	k	
ft	-0.52	ksi	okay
fb	-4.82	ksi	not okay,>.3f'ci

Release Stesses @ 60 db

fse	175.55	ksi	
Fse	2209.51	k	
ft	0.69	ksi	not okay,>6sqrt(f'ci)
fb	-5.75	ksi	not okay,>.7f'ci

Debonding

Try	50.00	strands	
e	13.61	in	
ES	26.95	ksi	
fse	175.55	ksi	
Fse	1904.75	k	
ft	0.34	ksi	okay
fb	-4.74	ksi	okay
x	4.00	ft	okay

Fatigue

γ(Δfps)	0.54	ksi	
ΔFth	18.00	ksi	okay

Ultimate Capacity

dp	58.00	in	
fps	270.00	ksi	
a	5.63	in	
ϕMn	15424.65	k-ft	okay

The stress diagrams at midspan are as follows:

Figure 29-Type IV, beam weight and slab weight midspan stresses at service

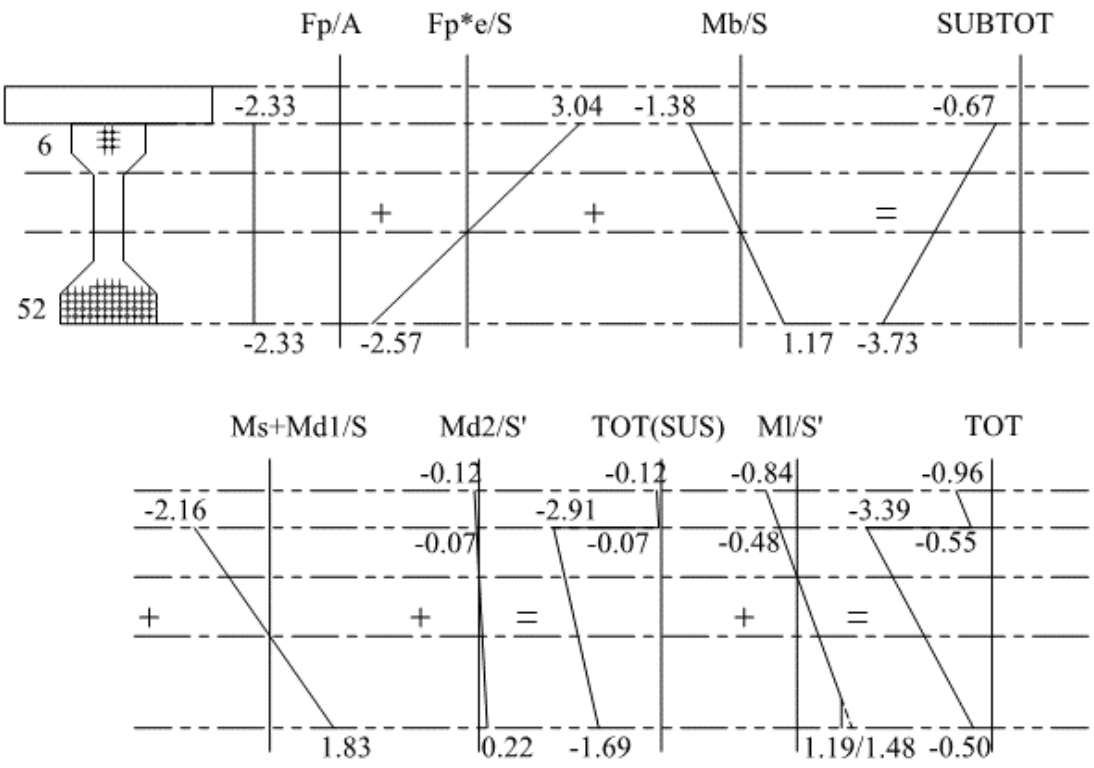

Figure 30-Type IV, beam weight and slab weight release stresses at 60db from ends (a) without debonding and (b) with debonding.

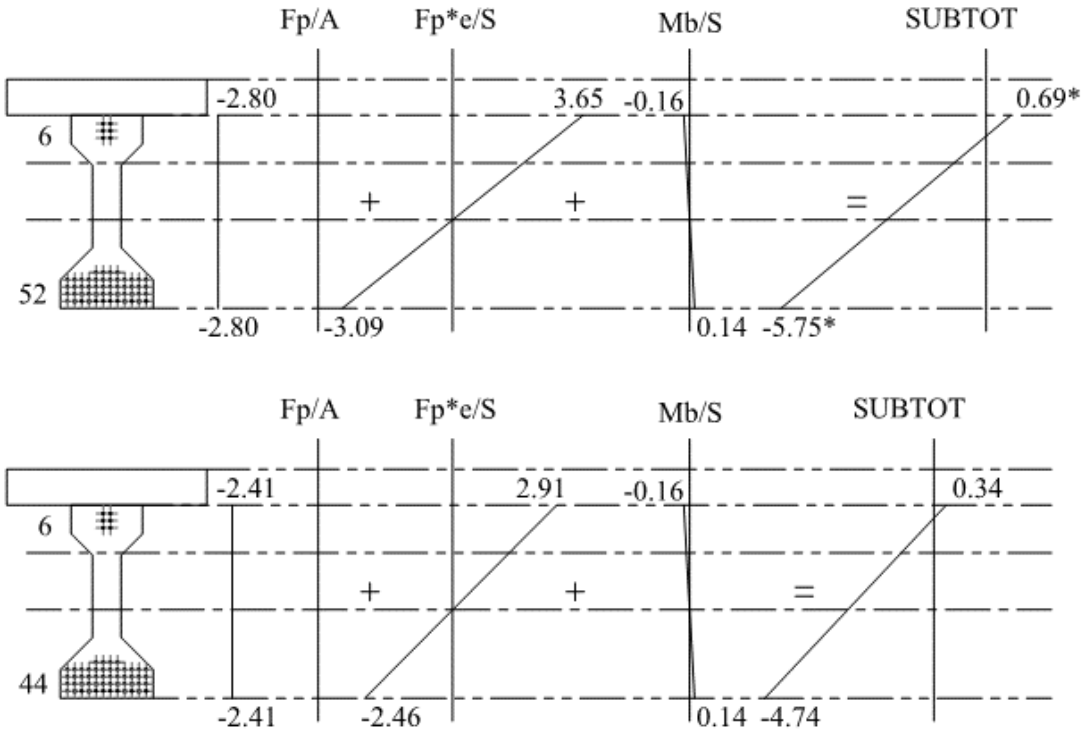

Debonding was required to reduce release stresses near the ends, 8 strands must be shielded for a minimum length of 5 feet. Also, the release stresses at midspan were slightly over code allowable (-4.82 ksi compared to -4.80 ksi allowable).

Camber and deflections are shown below:

PCI Method

	Non-cracked	
Initial Camber	4.74	in
Initial Deflection	-1.47	in
Initial Total	3.27	in
Camber @ Erection	8.54	in
Deflection @ Erection	-2.72	in
Subtotal @ Erection	5.82	in
Deflection Slab	-1.70	in
Deflection Dead 1	-0.22	in
Deflection Dead 2	-0.14	in
Total @ Erection	3.75	in
Camber System	10.44	in
Delfection System	-8.54	in
Total System	1.90	in
Deflection Live	-0.95	in
Total	0.95	in

+ upward

Dead	l/240	5.00	in
Live	l/800	1.50	in

The results of both the Type IV girder is summarized in the table below:

Bridge Girder Design Comparison (AASHTO Type IV Girder)					
	Girder Design				
	ODOT	Load Balance Beam Only	Load Balance Beam+0.5Slab	Load Balance Beam+0.75Slab	Load Balance Beam+1.0Slab
# of Prestressing Strands at bottom/ top	40/6=46	16/2=18	34/2=36	40/4=44	52/6=58
# of Mild Steel #9 Bars	0	6 @ bot	2 @ top, near ends	1 @ top, near ends	0
e @ Midspan, in.	14.64	18.29	18.17	16.09	14.73
Prestressing Release Force @ 60db, k	1803.70	749.2	1420.35	1719.12	2209.51
Total Prestressing Force @ Midspan	1529.5	669.6	1224.8	1462.21	1840.61
# of Debonding strands/ length	4/4’,2/8’,2/16’	0	Use mild steel	Use mild steel	8/4’
Total Stresses at Midspan	fb=0.34, ft=-3.53	fb=2.39*, ft=-3.57	fb=0.74, ft=-3.15	fb=0.32, ft=-3.31	fb=-0.50, ft=-3.39
Release Stresses at 60db, ksi before debonding	fb=-4.65, ft=0.52*	fb=-2.11, ft=0.43	fb=-4.11, ft=0.94*	fb=-4.67, ft=0.77*	fb=-5.75*, ft=0.69*
ϕMn, k-ft Mu=7310.7	11709.0	7620.1	8192.4	13646.3	15424.7
Release Camber	3.71	2.01	3.78	4.04	4.74
Net Total Δ, in.	-1.03	-5.07	-1.17	-0.60	0.95
Crack Width, in.	0.002	0.015	0.005	0.002	0.000
Fatigue	OK	OK	OK	OK	OK

Table 11

The load balancing designs for the Type IV girders demonstrate that by placing the prestressing force in an optimum location to counteract the gravity dead load, less prestressing strands are required to achieve the same level of stresses as a typical ODOT design. Load balancing just the beam weight is not ideal because a large portion of the dead load is ignored and thus large unbalanced loads exist. This design also creates large tensile stresses at midspan that vastly exceed allowable stresses. Additional mild steel is required to increase the ultimate bending capacity. Load balancing of the beam and half the remaining pre-composite dead load is comparable to the ODOT design, but with less prestressing strands. The situation of load balancing the entire pre-composite dead load requires too much prestressing and exceeds allowable stress limits during release that cannot be mitigated. Thus, a load balance design between the latter two designs would be the most advantageous while still meeting code requirements. Load balancing three quarters of the deck weight is the most efficient design by using less prestressing strands and reducing final stresses. Any tensile stresses at release can be mitigated with the use of a few mild steel bars near the ends. This is the most efficient design for providing uniform compressive stress under dead load while complying with code and requires no debonding.

Load balancing provides a precise location to place prestressing strands in order to balance the beam weight and some portion of the remaining dead load unique to every situation. This allows less prestressing to be used in comparison to designs that ignore load balancing and at a minimum are code compliant. This efficient use of material will save expensive high performance material and save on the total amount of debonding required. The lower required prestress force also helps reduce end region stresses with less debonding to limit end region cracking, creates tolerable camber and deflections, and uses less material.

CHAPTER V

CONCLUSIONS

The load balancing method for prestressed concrete members is a design method first proposed by T.Y. Lin. The first model proposed harping the prestressing strands in a parabolic pattern mirroring the moment diagram. This is readily achieved for post-tensioned members, but is not common practice for precast, prestressed members where straight strands are preferred. Also, parabolic draping works well when the load is nearly all dead load and when the geometric shape allows for the draping. However, this method must be adapted for long span bridge girders where dead load is added incrementally. This can be achieved by placing the straight strands in a strategic location and using debonding strands varying lengths to achieve a similar effect of draping the prestressing forces. The underlying goal of load balancing is to create a uniform compressive load along the length of the member in order to reduce tensile stresses and reduce induced curvature.

Load balancing is shown to be an efficient design method in reducing overall prestressing strands while meeting current codes. This efficiency is due to the location of the prestressing force to "balance" the beam weight and a portion of the remaining dead load ($M_d = F_p \times e$). The portion of the remaining dead load is variable, but should be the highest percentage possible while still achieving tolerable stresses and strength requirements. When straight strands are utilized, debonding is required to reduce stresses near the ends, as well as creating a similar effect to draping, or mild steel can be added to counteract any tensile stresses. The Type IV girder's

geometric properties allow prestressing to be placed with an ideal eccentricity, making loading balancing the design method of choice. Load balancing is a preferred design method to reduce prestressing force, create the most uniform compressive stresses under sustained loads, and still be code complaint.

Load balancing as a design method is applicable as an efficient design method for modern prestressed bridge girders. The method from T. Y. Lin is modified for long span members with large dead and live load applications. The load balancing method is effective at reducing susceptibility to cracking, lowering the amount of debonding, and lowering the total amount of prestressing strands. An efficient design for typical bridge girder design is made possible with the load balancing design method.

CHAPTER VI

RECOMMENDATIONS

The results of the thesis lend the following recommendations. Use load balancing for design of precast, prestressed bridge girders by balancing the girder self weight plus 75% of the cast-in-place concrete deck. When trying to balance 100% of the total dead load, stresses and initial cambers were excessive. This occurs because over half of the dead load is yet to be placed at the time or prestressing.

REFERENCES

ACI Committee 224. (2001). *Control of Cracking in Concrete Structures (ACI224R-01).*

ACI Committee 318. (2014). *Building Code Requirements for Structural Concrete (ACI 318-14).*

American Association of State Highway and Transportation Officials. (2010). *AASHTO LRFD Bridge Design Specifications* (Vol. 5th). Washington, DC.

Lin, T. (June 1963). Load-Balancing Method for Design and Analysis of Prestressed Concrete Structures. *Journal of the American Concrete Institute*, 719-742.

Lin, T., & Burns, N. H. (1981). *Design of Prestressed Concrete Structures* (Vol. 3rd). John Wiley & Sons, Inc.

Naaman, A., & Siriaksom, A. (March-April 1979). Serviceability Based Design of Partially Prestressed Beams. *PCI Journal*, 64-89.

Okumus, P., & Oliva, M. G. (Spring 2013). Evaluation of crack control methods for end zone cracking in prestressed concrete bridge girders. *PCI Journal*, 91-105.

Precast/Prestressed Concrete Institute. (2010). *PCI Design Handbook* (Vol. 7th).

Shaikh, A., & Branson, D. (February 1970). Non-tensioned Steel in Prestressed Concrete Beams. *PCI Journal*, 14-36.

Tadros, M. K., Fawzy, F., & Hanna, K. E. (Winter 2011). Precast, prestressed girder camber variability. *PCI Journal*, 135-154.

Zia, P., Kowalski, M. J., Ellen, G. C., Longo, S. E. (February 2003). Fatigue Testing of Two Full-Size Pre-Cracked AASHTO Bridge Girders. *Special Publication* (Volume 211), 1-16.

APPENDICES

Appendix A.1- Full Spreadsheet Printout Example

Beam Properties

Area	789.00	in^2
Yt	29.27	in
Yb	24.73	in
I	260730.00	in^4
St	8907.76	in^3
Sb	10543.07	in^3
V/S	4.90	in
Depth	54.00	in
Length	100.00	ft
Slab t	8.00	in
Spacing	11.33	ft

Material Properties

fps	270.00	ksi
fs	60.00	ksi
fci	7.00	ksi
fc	10.00	ksi
f'c slab	4.50	ksi
Es	29000.00	ksi
Eps	28500.00	ksi
Eci	4820.75	ksi
Ec	5761.90	ksi
Eslab	3865.20	ksi
db	0.60	in^2
Aps	0.22	in^2
β1	0.65	

Transformed Properties

838.37	in^2	
30.13	in	
23.87	in	
270690.53	in^4	
8983.44	in^3	
11341.24	in^3	
n	4.95	

Deck Transformed Properties

1518.64	in^2	
21.29	in	
40.71	in	
684221.68	in^4	
32145.35	in^3	
16805.25	in^3	
n	0.67	

Cracked Properties

A'	0	in^2
g'	10	in
db	1	in
n	5.03	
k	0.30	

Input
Calc.
okay
not okay

Precomposite

Mcr	4228.15	k-ft
Icr**	152697.49	in^4
Ieff	260730.00	in^4

**AASHTO Type IV only

Composite

6364.24	k-ft	
170851.16	in^4	
684221.68	in^4	

Loads

Self	0.822	klf
Slab	1.133	klf
Dead 1	0.150	klf
Dead 2	0.250	klf
Live	1.660	klf

Moments @ Midspan

Self	1027.34	k-ft
Dead 1	1603.75	k-ft
Dead 2	312.50	k-ft
Live	2075.00	k-ft
Md	2943.59	k-ft
Ml	2075.00	k-ft

Ma	5018.59	k-ft
Mu	7310.74	k-ft

Moments @ 60db

119.58	k-ft
186.68	k-ft
36.38	k-ft
241.53	k-ft
342.63	k-ft
241.53	k-ft

584.16 k-ft

Ultimate Capacity

dp	57.25	in	
fps	270.00	ksi	
a	4.28	in	
ϕMn	11709.00	k-ft	okay

Preliminary Design

g (guess)	4.40	in
e	20.33	in
fse(guess)	152.00	ksi
N	37.47	strands
Try	46.00	strands
g	10.09	in
e	14.64	in
e@60db	14.64	in

Preliminary Total Stresses @ Midspan

fb	-0.15	ksi	okay
fr(7.5)	0.75	ksi	

Total Stresses @ Midspan

fse	153.23	ksi			
Fse	1529.52	k			
fp/A	-1.94				
fpe/Sb	-2.12				
M1/Sb	2.99		1.17		1.83
M2/S'b	0.22				
Ml/S'b	1.19		-0.84		
fb	0.34	ksi		okay	
fpe/St	2.51				
M1/St	-3.54		-1.38		-2.16
M2/S't	-0.07				
Ml/S't	-0.48				
ft(sust)	-3.04	ksi		okay	
ft(tot)	-3.53	ksi		okay	

Release Stresses @ Midspan

fse	183.91	ksi	
Fse	1835.84	k	
ft	-0.69	ksi	okay
fb	-3.71	ksi	okay

Release Stesses @ 60 db

fse	180.70	ksi	
Fse	1803.70	k	
ft	0.52	ksi	not okay
fb	-4.65	ksi	okay

Total Stresses @ 60db

fse	148.00	ksi	
Fse	1477.37	k	
fb(sust)	-3.55	ksi	okay
fb(tot)	-3.41	ksi	okay
ft	0.08	ksi	okay

Debonding

Try	38.00	strands	
e	13.15	in	
ES	21.80	ksi	
fse	180.70	ksi	
Fse	1490.02	k	
ft	0.15	ksi	okay
fb	-3.61	ksi	okay
x	2.00	ft	okay

Crack Width (ACI 224R)

w	0.002	in	okay

Bonded Reinforcement Req'd

c	2.15	in
T	3.23	k
As req'd	0.05	in^2

Spacing (AASHTO)

s	841.32	in	okay
βs	2.43		

Fatigue

γ(Δfps)	0.54	ksi	
ΔFth	18.00	ksi	okay

AASHTO Loss Method (Midspan)

Δf_{ES}	18.59	ksi	9.18	%
Approximate				
Δf_{pLT}	25.54	ksi	12.61	%
Δf_{pT}	44.13	ksi	21.79	%
Refined				
Before Deck				
Δf_{pSR}	5.80	ksi	2.86	%
Δf_{pCR}	11.36	ksi	5.61	%
Δf_{pR1}	1.27	ksi	0.63	%
Δf_{pdT}	18.42	ksi	9.10	%
After Deck				
Δf_{pR2}	1.27	ksi	0.63	%
Δf_{pSD}	8.42	ksi	4.16	%
Δf_{pCD}	0.00	ksi	0.00	%
Δf_{pSS}	2.57	ksi	1.27	%
Δf_{pLT}	30.69	ksi	15.15	%
Δf_{pT}	49.27	ksi	24.33	%

Supplemental Parameters

ϵ_{bid}	0.000241	
ϵ_{bdf}	0.000324	
ψ_b	0.724532	
ψ_{bif}	0.972812	
ψ_{bdf}	0.972584	
K_{id}	0.843282	
K_{bdf}	0.91208	
ti	7	days
td	100	days
tf	3650	days
RH	65	%
Δf_{cgp}	3.143689	
Δf_{cgpd}	1.67881	
ε_{ddf}	0.00047	
Δf_{cdf}	0.339279	
(V/S)d	4	

AASHTO Loss Method (60db)

Δf_{ES}	21.80	ksi	10.77	%
Approximate				
Δf_{pLT}	25.28	ksi	12.48	%
Δf_{pT}	47.08	ksi	23.25	%
Refined				
Before Deck				
Δf_{pSR}	5.80	ksi	2.86	%
Δf_{pCR}	13.56	ksi	6.70	%
Δf_{pR1}	1.17	ksi	0.58	%
Δf_{pdT}	20.53	ksi	10.14	%
After Deck				
Δf_{pR2}	1.17	ksi	0.58	%
Δf_{pSD}	8.42	ksi	4.16	%
Δf_{pCD}	0.00	ksi	0.00	%
Δf_{pSS}	2.57	ksi	1.27	%
Δf_{pLT}	32.69	ksi	16.14	%
Δf_{pT}	54.50	ksi	26.91	%

Supplemntal Parameters

ϵ_{bid}	0.000241
ϵ_{bdf}	0.000324
ψ_b	0.724532
ψ_{bif}	0.972812
ψ_{bdf}	0.972584
K_{id}	0.843282
K_{bdf}	0.91208
Δf_{cgp}	3.755339
Δf_{cgpd}	3.245284
ε_{ddf}	0.00047
Δf_{cdf}	0.339279
(V/S)d	4

PCI Loss Method (Midspan)

fcir	3.11	ksi		
ES	18.38	ksi	9.08	%
CR	23.28	ksi	11.50	%
SH	5.77	ksi	2.85	%
RE	3.10	ksi	1.53	%
TL	50.54	ksi	24.96	%

PCI Loss Method (60db)

fcir	3.72	ksi		
ES	22.00	ksi	10.86	%
CR	35.94	ksi	17.75	%
SH	5.77	ksi	2.85	%
RE	2.45	ksi	1.21	%
TL	66.16	ksi	32.67	%

Input

Fp	1835.84	k
Fp'	1529.52	k
e	14.64	in
e'	30.62	in
L	100.00	ft
Ec	5761.90	ksi
Eci	4820.75	ksi
I	270690.53	in^4
I'	684221.68	in^4
Ieff	260730.00	in^4
Ieff'	684221.68	in^4
ϕ	2.05962E-05	in^-1
ϕ28 days	1.7232E-05	in^-1
ϕcomp	1.18813E-05	in^-1
Self	0.82	klf
Slab	1.13	klf
Dead 1	0.15	klf
Dead 2	0.25	klf
Live	1.66	klf

PCI Method

	Non-cracked	
Initial Camber	3.71	in
Initial Deflection	-1.42	in
Initial Total	2.29	in
Camber @ Erection	6.67	in
Deflection @ Erection	-2.62	in
Subtotal @ Erection	4.05	in
Deflection Slab	-1.63	in
Deflection Dead 1	-0.22	in
Deflection Dead 2	-0.14	in
Total @ Erection	2.06	in
Camber System	8.16	in
Delfection System	-8.24	in
Total System	-0.08	in
Deflection Live	-0.95	in
Total	-1.03	in

+ upward

Dead	l/250	4.80	in
Live	l/800	1.50	in

PCI Method @ 1/10th Points

x (ft)	0	3	10	20	30	40	50
Self Moment	0.00	119.58	369.84	657.50	862.97	986.25	1027.34
Dead 1+Slab Moment	0.00	186.68	577.35	1026.40	1347.15	1539.60	1603.75
Dead 2 Moment	0.00	36.38	112.50	200.00	262.50	300.00	312.50
Live Moment	0.00	241.53	747.00	1328.00	1743.00	1992.00	2075.00
N	40	40	44	46	46	46	46
e	13.15	13.15	13.87	14.64	14.64	14.64	14.64
fcir	3.054	2.982	3.253	3.358	3.220	3.137	3.109
ES	18.06	17.63	19.23	19.85	19.03	18.54	18.38
CR	30.21	28.72	29.63	28.44	25.57	23.85	23.28
SH	5.77	5.77	5.77	5.77	5.77	5.77	5.77
RE	2.84	2.92	2.81	2.84	2.98	3.07	3.10
TL	56.88	55.03	57.46	56.90	53.37	51.24	50.54

Fp @ Release	1600.97	1604.69	1749.83	1823.18	1831.35	1836.25	1837.89
Camber	0.00	0.35	1.25	2.45	3.23	3.70	3.85
Deflection	0.00	-0.14	-0.46	-0.87	-1.20	-1.40	-1.47
Subtotal	0.00	0.21	0.79	1.57	2.03	2.29	2.38
ft	0.33	0.17	0.01	-0.20	-0.47	-0.64	-0.69
fb	-4.03	-3.90	-4.10	-4.09	-3.88	-3.75	-3.71

Fp @ Deck Cast	1263.96	1280.01	1384.88	1453.37	1488.66	1509.84	1516.90
Camber@erection	0.00	0.63	2.25	4.40	5.81	6.65	6.94
Deflection@erection	0.00	-0.44	-1.46	-2.76	-3.78	-4.42	-4.64
Subtotal	0.00	0.19	0.79	1.65	2.03	2.23	2.29
ft	0.26	-0.15	-0.87	-1.72	-2.42	-2.83	-2.97
fb	-3.18	-2.87	-2.50	-1.94	-1.44	-1.14	-1.03

Fp @ composite	1263.96	1280.01	1384.88	1453.37	1488.66	1509.84	1516.90
Camber @ composite	0.00	0.77	2.75	5.38	7.10	8.13	8.48
Deflection	0.00	-0.82	-2.68	-5.07	-6.94	-8.13	-8.54
Subtotal	0.00	-0.04	0.07	0.31	0.15	0.00	-0.06
Live load Deflection	0.00	-0.09	-0.30	-0.56	-0.77	-0.90	-0.95
Total	0.00	-0.13	-0.22	-0.25	-0.62	-0.90	-1.01
ft (sustained)	0.26	-0.15	-0.90	-1.77	-2.48	-2.90	-3.05
ft (total)	0.26	-0.21	-1.08	-2.08	-2.88	-3.37	-3.53
fb	-3.18	-2.71	-1.99	-1.04	-0.26	0.22	0.37

Stand Location Calculation

Strands		Inches from bottom		
12	@	2	=	24
12	@	4	=	48
12	@	6	=	72
2	@	8	=	16
0	@	10	=	0
0	@	12	=	0
0	@	14	=	0
0	@	16	=	0
0	@	18	=	0
0	@	20	=	0
0	@	22	=	0
0	@	24	=	0
0	@	26	=	0
0	@	28	=	0
0	@	30	=	0
0	@	32	=	0
0	@	34	=	0
0	@	36	=	0
0	@	38	=	0
0	@	40	=	0
0	@	42	=	0
0	@	44	=	0
0	@	46	=	0
0	@	48	=	0
0	@	50	=	0
0	@	52	=	0
Σ 38			Σ 160	in^2
			g 4.21	in

Truck Live Load Moment

Front Wheel	8.00	k
Mid Wheel	32.00	k
Rear Wheel	32.00	k
Span	100.00	ft
Distance 1-2	14.00	ft
Distance 2-3	14.00	ft
x bar	18.67	ft
Distance to 1	33.67	ft
Reaction L	34.32	k
Moment	1523.92	k-ft
w	1.22	klf
Multi-pres.	1.00	
Lane Load	0.64	klf
Dynamic F	1.33	
Distribution	0.73	
w use	1.66	klf

Load Balancing Method Md=Fp*e

ws	0.822	klf
wd	1.125	klf
L	100	ft
Ase	0.217	in^2
fse	150	ksi
yb	24.73	in

Load Balance Method 1
Beam Only

n	20	
e	18.94	in
g	5.79	in

Load Balance Method 2
Beam+0.5*Slab

n	32	
e	19.94	in
g	4.79	in

Load Balance Method 3
Beam+1.0*Slab

n	46	
e	19.51	in
g	5.22	in

VITA

Lance R. Luke

Candidate for the Degree of

Master of Science

Thesis: LOAD BALANCING AS A DESIGN METHOD FOR CONCRETE PRESTRESSED BRIDGE GIRDERS

Major Field: Civil Engineering

Biographical:

Education:

Completed the requirements for the Master of Science in Civil Engineering at Oklahoma State University, Stillwater, Oklahoma in December, 2016.

Completed the requirements for the Bachelor of Science in Architectural Engineering at Oklahoma State University, Stillwater, Oklahoma in May, 2012.

Experience: Practiced engineering at Kirkpatrick Forest Curtis, PC since undergraduate degree in 2012.

Professional Memberships: Member of Oklahoma Structural Engineers Association, National Structural Engineers Association, ACI, and a student member of PCI.